ISSN 0110–3326

RESEARCH REPORT

Axial Behaviour of Bored Pile Foundations

K. J. McManus

January 1997

97-2

Department of Civil Engineering

University of Canterbury
Christchurch New Zealand

AXIAL BEHAVIOUR OF BORED PILE FOUNDATIONS

EQC 95/184

Final Report, January 1997

Prepared by

UNIVERSITY OF CANTERBURY
Department of Civil Engineering
Christchurch
New Zealand

Research Report 97-2

Author and Principal Investigator
K. J. McManus

Prepared for
Earthquake Commission
Box 311
Wellington
New Zealand

Director of Research Fund
R. I. Skinner

Abstract

Nine bored pile foundations, each nominally 0.75 m diameter by 5.5 m deep, were constructed in a deposit of loose gravel above the water table. Four of the piles were loaded monotonically to failure in uplift while the remaining five were subjected to 30 cycles of 1 Hz sine wave loading at various amplitudes prior to being failed in uplift. The uplift capacity and stiffness of the cyclically loaded piles was compared with that of the monotonically loaded piles. At low levels of cyclic loading (less than 60 percent of uplift capacity) the pile response was largely elastic with no significant degradation in stiffness. At higher levels, the pile response was highly inelastic and non-linear with a large reduction in load-displacement stiffness (by a factor of up to 16.1). These results are in general agreement with an equivalent study carried out at model scale in the laboratory, providing evidence that such model studies may be useful in predicting prototype response to cyclic loading. Recommendations for practice are made.

Acknowledgements

This project was funded principally by the Earthquake Commission under research grant EQC 95/184. The University of Canterbury provided some additional funding and much of the equipment. The Selwyn District Council made available the test site.

This project has truly been a team effort and many people have contributed in different ways, not all of whom are mentioned below. Ray Allen fabricated the actuator swivels and heavy plates, Tony Vreughdenhill fabricated the load frame, and John van Dyk made everything work on site. Roger Vreughdenhill did the initial site selection leg work, and Al Chambers assisted with running the tests. Richard Newton came to the rescue when the load cell failed. Val Grey prepared some of the figures.

Contents

Introduction

Many structures in New Zealand are supported on foundations consisting of two or more bored piles. During an earthquake, these piles are subjected to cyclic axial loading of various magnitudes depending on the geometry of the structure, as shown in Figure 1. In many cases, net uplift loading of the foundation will result. The effect of cyclic axial loading on the stability of the bored pile foundations is poorly understood but of considerable concern [1].

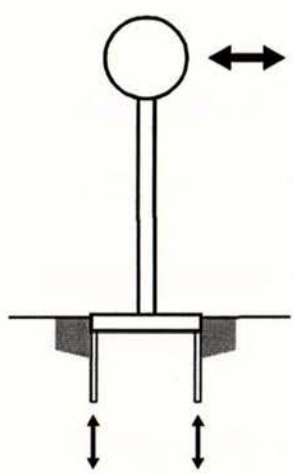

Figure 1. Earthquake induced axial loads on bored piles.

Observations after the 1985 Mexico City earthquake [2] indicated that some 25 buildings supported on friction piles suffered sudden settlements during the earthquake. At least one building overturned [3], with several of the friction piles having pulled out of the soil. Zeevaert [4] concluded that cyclic axial loading during the earthquake mobilized the side capacity of the piles allowing plunging deformation to occur. It is not clear from these observations, however, whether the failures were caused by simple overloading of the piles by the earthquake induced axial forces, or by degradation of the side friction capacity of the piles during cyclic loading.

A recent review of the available published data concerning repeated load tests on deep foundations [5] showed the following: (a) all but the very lowest levels of repeated axial loading (as low as 10 to 20 percent of the static capacity in a few reported studies) show continuing deformation without any apparent limit, (b) repeated two-way or one-way uplift loads generally lead to capacity reductions, while repeated one-way compression loads have less effect on capacity, and (c) repeated loads producing axial displacements greater than about 5 percent of the pile diameter may be required to cause static capacity reductions.

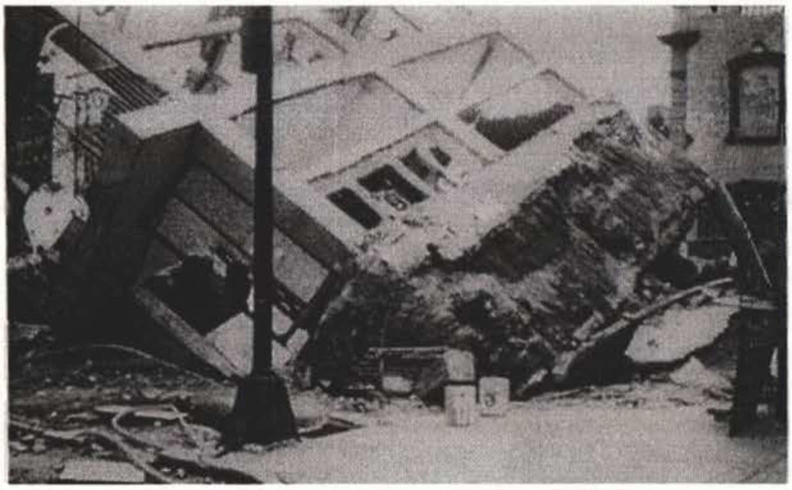

Figure 2. View of collapsed building.
Source: Mendoza and Auvinet [3]

Few field or laboratory data were available at that time for bored pile foundations. More data were available for driven piles, although the applicability of driven pile results for predicting the response of bored piles to cyclic loading is uncertain because of considerable differences in geometry and method of installation. However, two recent experimental studies [6, 7] have provided some insights and data for bored pile foundations which are of relevance to aseismic design.

Both experimental studies were sponsored by the electric power industry with a focus on wind induced cyclic loading of transmission structures. Therefore, the frequencies of cyclic loading studied were somewhat lower than for earthquake loading (0.02 - 0.2 Hz compared with 1 Hz for a typical bridge structure) and the duration of cyclic loading was somewhat greater (11 - 300 cycles compared with 5 - 20 for a typical earthquake situation). However, these differences are not believed to be so significant as to preclude interpretation of the results for aseismic design situations.

For the first study [6], model bored piles of 76 and 152 mm diameter and depth to diameter ratios (D/B) of 4 to 8 were tested in loose, medium, and dense filter sand. The results may be summarised as follows: (a) For the cyclic load tests at low values of LRL (level of repeated load defined as cyclic load amplitude plus mean load normalised by pile side friction capacity), the displacement response typically remained stiff and linear-elastic with no discernible deterioration from the static load-displacement response. In such cases there was either no significant change or a slight increase in capacity. (b) At higher values of LRL, the displacement response typically degraded to a much softer, hysteretic behaviour. In such cases there was a significant decrease in capacity. (c) At still higher values of LRL, the displacement response typically degraded very rapidly with the pile pulling out before application of the full 100 cycles.

For each different soil condition and pile geometry, a critical level of repeated load (CLRL) was determined by considering the level of repeated load (LRL) required to cause the model bored piles to pull out in 100 cycles or less. The resulting values of CLRL are shown in Table 1. Values of CLRL ranged from 0.08 (i.e. 8 percent of the side friction capacity of the pile applied as a repeated load caused pullout in less than 100 cycles) to greater than 0.65.

Table 1. Critical Level of Repeated Load for Model Bored Piles in Sand
Source: Turner and Kulhawy [6]

Soil	CLRL	
condition	D/B=4	D/B=8
Loose	>0.65	0.24-0.47
Medium	0.27-0.42	0.15-0.26
Dense	0.38-0.46	0.08-0.14

For the second study [7], model bored piles were constructed with diameters of 59, 89, and 174 mm and depth to diameter ratios of 6.7 and 4.0 in laboratory prepared deposits of clay. Patterns of response were similar to those described above for the model piles in sand. Values of CLRL were determined for each different soil condition (clay deposits were either highly overconsolidated or had a low overconsolidation ratio of 1.8) and pile geometry and are shown in Table 2. Values of CLRL ranged from as low as 0.12 to 0.37.

Table 2. Critical Level of Repeated Load for Model Bored Piles in Clay
Source: McManus and Kulhway [7]

Soil condition	CLRL	
	D/B=4	D/B=6.7
Low OCR	-	0.24-0.37
High OCR	>0.27	0.12-0.25

The concept of the cyclic stability diagram, shown in Figure 3, was introduced by Poulos [8]. This diagram summarises the change in foundation capacity with cyclic axial loading for the complete range of possible combinations of mean and cyclic components of load, from one-way in uplift to two-way to one-way in compression. Three regions within the diagram are identified: (a) a stable zone in which cyclic loading has no effect on foundation capacity, (b) a metastable zone in which cyclic loading causes some limited reduction in capacity, and (c) an unstable zone in which cyclic loading will result in failure within a specified number of cycles. The cyclic stability diagram was used to aid interpretation of results in the second model study described above.

Pender [1] reported on a thorough overview of aseismic pile design and analysis techniques. He stated that accurate assessment of the vertical capacity of piles under cyclic loading is required for design purposes and that the cyclic vertical capacity is likely to be significantly less than the static capacity. However, no suitable method for assessing the degradation in cyclic axial capacity of bored piles was identified and this was listed as an area requiring further research.

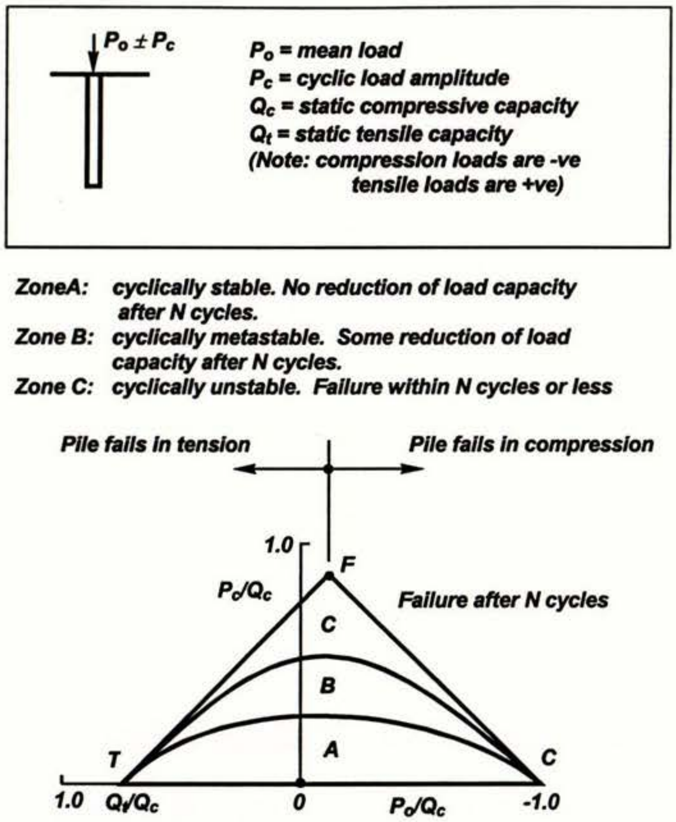

Figure 3. The Cyclic Stability Diagram.
Source: Poulos [8]

Since this report was published, McManus and Turner [9] have demonstrated a simple approach for predicting foundation response by using the above mentioned model study results to predict directly the amount of degradation in side resistance that may occur during an earthquake. For the example of a typical highway bridge structure founded on pairs of bored piles, they concluded that degradation in side resistance was likely to occur resulting in loss of equilibrium and a crude rocking motion. Overturning of the structure was found to be unlikely, with permanent settlement of 40 to 50 mm being the most significant result.

More recently, a further model study has been completed at the University of Canterbury [10]. Essentially, the study of Turner and Kulhawy [6] was repeated but using frequencies of loading (1 Hz) and numbers of cycles (30) chosen to better simulate earthquake events. Model bored piles of 95 mm diameter by 1450 mm long were constructed in 1 m diameter by 2 m deep laboratory prepared deposits of loose sand (relative density D_r = 14 percent). A mean dead load was applied to each model bored pile and then a simulated earthquake, consisting of 30 cycles of sine wave loading at 1 Hz, was applied. Immediately after the "earthquake", each pile was failed in uplift. Any change in pile uplift capacity was determined by comparing the measured capacity with that of several piles which were load tested without any cyclic loading.

All of the piles responded to the cyclic loading by "walking" downwards into the soil, even when the mean applied load was in uplift. At modest levels of cyclic loading, the total downwards displacement was only a few millimetres or less and the pile uplift capacity, measured on completion of the simulated "earthquake", was found to be unchanged. Some combinations of mean and cyclic load caused the piles to fail in uplift, while other combinations caused the piles to fail in compression. All of the load test results are summarised on the cyclic stability diagram shown in Figure 4.

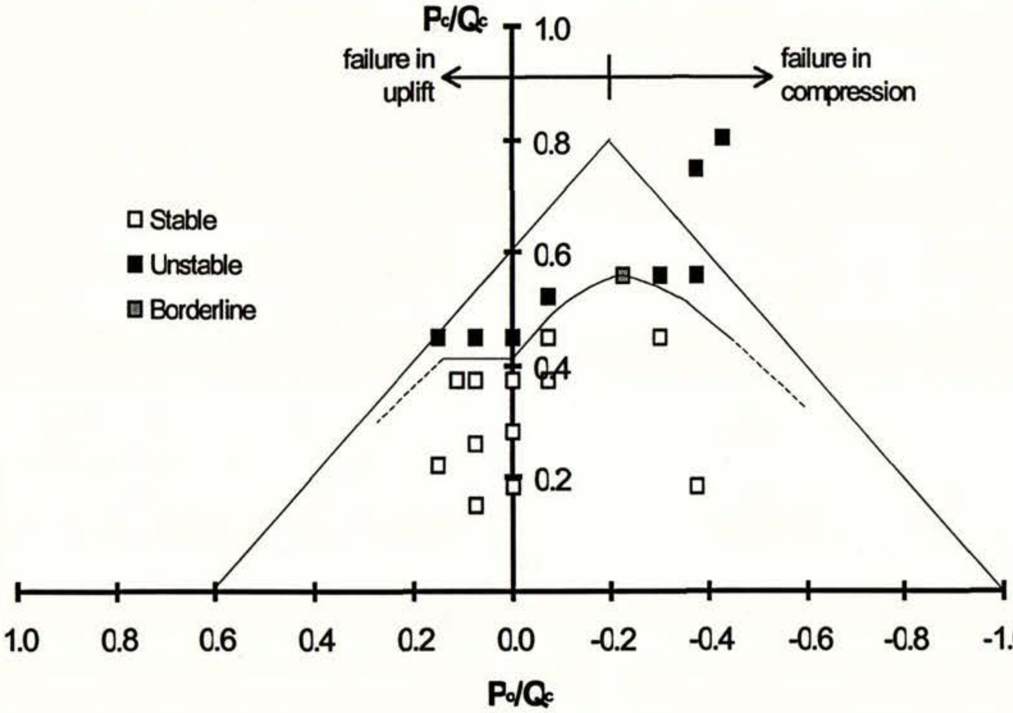

Figure 4. Cyclic stability diagram for model bored piles with simulated earthquake loading.

Source: McManus and Chambers [10].

A pronounced dip in the stable/unstable boundary is evident where it crosses the $P_o/Q_c = 0$ axis (i.e. zero mean load). In other respects, the diagram largely follows the idealised shape predicted by Poulos [8]. The significance of this dip in the diagram is that the worst case for cyclic loading occurred when zero mean load was applied to the piles. For this condition, the stable/unstable boundary defines a critical level of repeated load (CLRL = 0.67). Applying cyclic axial load of more than 67 percent of pile uplift capacity caused instability to occur, while below this level all piles remained stable. Applying mean load in uplift did not reduce the amplitude of cyclic loading that the piles could sustain and applying mean load in compression increased it.

This present study is a necessary further step in the process of developing a reliable design methodology for aseismic design of bored piles. Model studies are accepted as a quick and economical way to explore qualitative patterns of response but direct extrapolation of quantitative results to full-size foundations is uncertain and unproved. The laws of dimensional analysis and similitude are not easily satisfied by model bored piles constructed in soil. If a linear dimension of the prototype is n times the equivalent dimension for the model, then the model must be tested in n times gravity in a centrifuge to obtain the correct distribution of gravity-induced stresses and soil stress-strain behaviour [11]. Therefore, it is not possible to develop formal equations to express the relationships between model and prototype quantities for the model studies referred to above. However, if such relationships could be established empirically by repeating a limited number of the model tests on full-size prototypes then the usefulness of the numerous model test results would be greatly extended.

The primary objective of this project, therefore, was to test the predictions from the above model studies for full-size bored piles by performing a limited number of full-size, cyclic load tests. To meet this objective it was desirable to match the model conditions as closely as possible including pile geometry, soil type, drainage conditions, load combinations, rate of loading, and number of cycles. As a secondary objective, the results from these tests should also provide valuable direct quantitative information regarding the performance of bored piles during cyclic axial loading, irrespective of the outcome of the primary objective. Stiffness data is also provided which should assist designers with predicting overall structural response to earthquake events.

From this information, the evaluation of risk to existing structures founded on multiple bored piles and the design of future foundations may be improved.

Site Selection

The first work phase involved securing a suitable site for the full-size bored pile tests. Two criteria were established as being most important in the selection process: (1) that the test site material be granular and homogeneous and (2) that the water table be well below the level of the base of the piles. A granular material was required because of the need to match the model conditions as closely as possible and because a granular soil (sand) was used for the laboratory model studies . Also, to maintain similarity of length scales between the laboratory and field, a field soil mean grain size (D_{50}) of 4 mm was desired, corresponding to a coarse sand-gravel site. A low water table was required, again, to match the laboratory model conditions where the soil was always dry. As an additional benefit, a low water table effectively increases the effective density of the soil by a factor of approximately 2 meaning that the test piles would represent piles of two times as large under more usual field conditions of a high water table.

Initial investigations focused on a coastal dune site, but these were eventually abandoned because of the shallow water table and the high residential population density of eastern Christchurch. Also, some reservations were held about siting the tests on the crest or plateau of an historical or present dune because of uncertainties regarding the effect of dune shape on in-situ soil stresses. A series of river-derived, inland sand dunes were investigated, but these tended to be elongated sand ridges of less than six metres in depth and were considered unsuitable.

Next, an investigation of the gravel formations surrounding Christchurch city was carried out. Inspection of several gravel extraction pits to the northwest of the city confirmed that the most geologically recent, fluvial gravels were very coarse and dense. At such sites, driving a pile casing was considered to be extremely difficult, possibly requiring pre-drilling ahead of the casing and thereby compromising pile uniformity. Experienced local drillers suggested that the material to the southwest of the city also was unsuitable for the project because of the presence of large amounts of fines in the soil and unstable water table fluctuations. However, regional geological maps and well-log data indicated a band of slightly older gravels running west of the city that appeared to be more suitable.

Finally, the investigations focused on a little used gravel pit immediately west of Christchurch city, close to the intersection of Jones Road and Curraghs Road approximately halfway between the settlements of Weedons and Templeton, as shown in Figure 5. The test site material is the Halkett member of the Springston Formation, of recent geologic age. The soil comprises fluvial gravel, sand, and a small fraction of silt, all largely derived from the degradation of older gravels (Waimakariri River sourced). Inspection of the exposed faces of the gravel pit indicated that the material was superficially uniform, with minimal layering. The depth to water table at the gravel pit was found to be in excess of eight metres, below the intended depth of the piles. Unfortunately, preliminary investigations at the test site immediately revealed the gravels to be very dense. If the bored piles were constructed in such dense material then the pullout loads would be excessive, beyond the means of reasonable experimental equipment to overcome. Therefore, it was necessary to loosen the material by excavating and re-depositing it using heavy earthmoving equipment

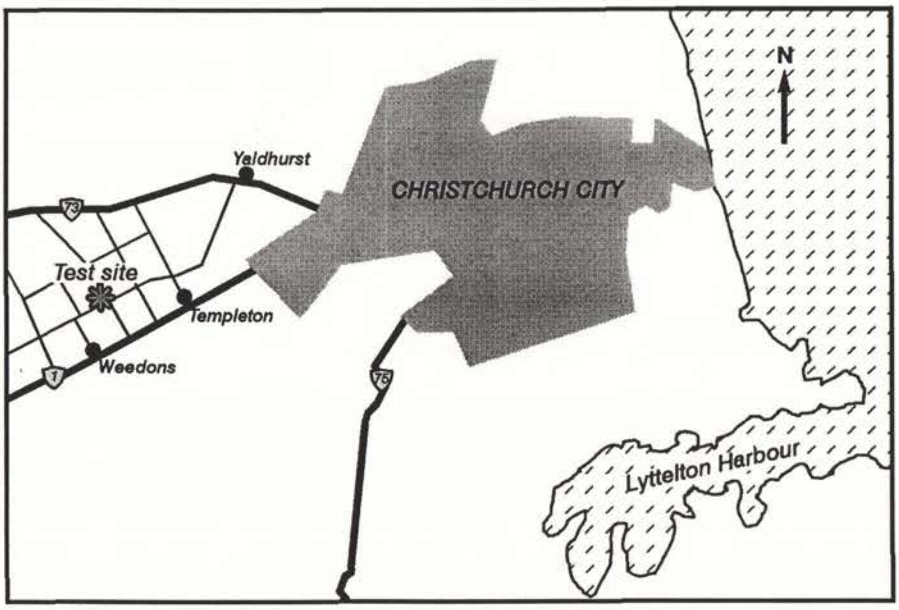

Figure 5. Location of Test Site.

Site Preparation

Extensive discussions and investigations led to the conclusion that the desired low water table, granular soil material, and low soil density were mutually exclusive properties, certainly in the Christchurch vicinity. Therefore, the decision was reached that the best solution would be to modify the in-situ soil density at the test site by mechanical means. A scheme was devised to excavate a large open pit at the Curraghs Road test site to a depth of 6 m and then to refill it using a large backhoe. Figures 6 and 7 show this work in progress. The test piles were then able to be constructed in the much looser material. The re-deposition of the material had benefits additional to reduction in density: The soil was mixed and re-deposited as a more uniform deposit, the soil gradation was better known, the soil in-situ stress state was better known, and any undesirable cementing of the soil was removed.

Figure 6. Test site during reworking of soil.

Figure 7. Excavation of test site.

Soil Properties

During the re-working of the site materials, field density tests were performed by having the backhoe deposit soil into large buckets simulating the re-deposition process. These buckets were then weighed and the soil moisture content determined by usual means. The friction angle, ϕ, for the material was determined by an in-situ, large-size shear-box test shown in progress in Figure 8. For such coarse material, field shear tests are a very practical way of measuring soil strength and have the added advantage of eliminating the uncertainty implicit in trying to re-compact the material to field condition in the laboratory. All of the known soil properties are summarised in Table 3. Particle gradation curves are given in Figure 9.

Table 3. Soil properties at Curraghs Road test site.

Property	**Symbol**	**Value**
Bulk unit weight	γ	17.2 KN/m^3
Dry unit weight	γ_d	16.4 KN/m^3
Moisture content	w	4.6 %
Mean particle size	D_{50}	15 mm
Friction angle	ϕ	43

Cone penetration tests (CPT) were carried out at the site after the re-deposition was completed by using the Department of Civil Engineering truck mounted drilling rig shown in operation in Figure 10. Two soundings were carried out on 29 February 1996 shortly after completion of the re-deposition and two further soundings were carried out on 28 May 1996 shortly before construction of the piles was commenced. The average value for q_c for the first soundings was approximately 2 MPa and this was unchanged for the later two soundings. This low value indicates a loose to very loose soil condition with relative density (I_d) of approximately 20 percent. All of the CPT soundings are shown in Appendix B.

Standard penetration tests (SPT) were made by Canterbury Drilling Company with average values reported of N = 1 with their full report included as Appendix C. On site observations indicated that these tests were not performed in accordance with standard procedure, a conical probe was used instead of a split spoon sampler and the soundings were made at the bottom of an open, large diameter, augured hole. The augur probably disturbed the soil being tested and the large diameter opening would have reduced the soil confinement, both effects contributing to a reduced blow count.

Figure 8. In-situ shear test in progress.

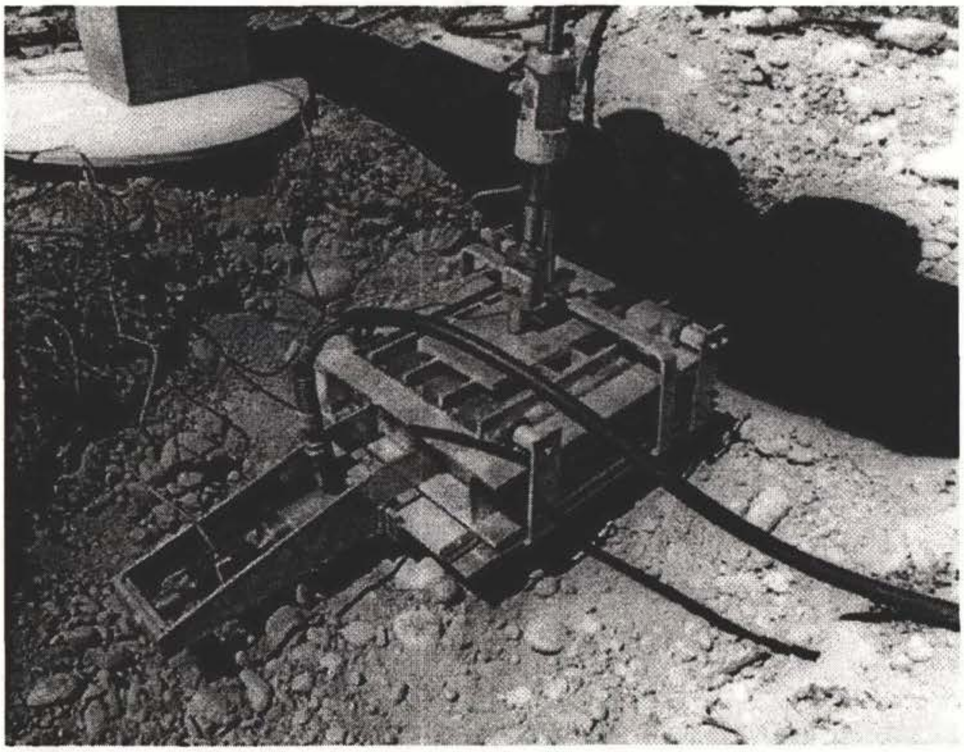

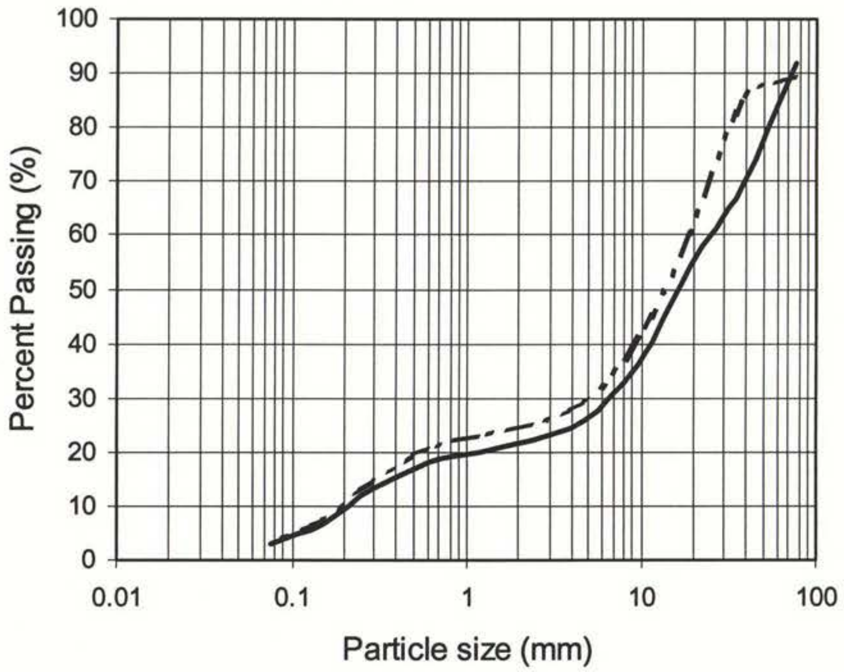

Figure 9. Particle gradation curves for test soil.

Pile Construction

Nine piles each of nominal size 750 mm diameter by 5.5 m deep were constructed on a three-by-three grid at 3.5 m spacing. The piles were constructed under contract by the Canterbury Drilling Company Ltd using a truck mounted Calweld bucket augur rig. First, a hole was bored to 2 m deep and then a temporary steel casing was stood and driven to the full depth of 5.5 m (Figures 11 and 12). Next, soil was removed from the inside of the casing using a bucket augur. This step proved to be the most time consuming as large size cobbles would get caught between the bucket and the casing causing the rig to stall frequently. The operator commented that a helical augur rig would have overcome this problem and would thus be more suitable for constructing bored piles in this soil type. Next the reinforcing cage was stood and set level in the hole ready to receive the concrete (Figure 13). Concreting proceeded in four steps: (a) concrete was poured to a depth of 2 m from the bottom of the hole, (b) the casing was pulled for about 1 m to make certain that it was not binding in the ground, (c) the remainder of the concrete was poured into the casing to a level of 1 m above the ground, and (d) the casing was pulled completely out of the ground (Figure 14). During the pulling of the casing the concrete level was observed to drop markedly, presumably because of a slight expansion of the hole under the pressure of the wet concrete. Finally, the concrete surface was struck off to the desired level and the protruding threaded portion of the reinforcing bars cleaned off.

Concrete strength was nominally of 20 MPa and the slump was measured at each pour with an average value of 170 mm. A high slump was chosen to facilitate pulling of the pile casing. The reinforcing cage consisted of four D24 bars and four D16 with a 10 mm spiral at 150 mm pitch. The four D24 bars were made 500 mm longer than the pile and were threaded on the ends to provide a connection to the loading system.

Figure 11. Truck mounted Calweld bucket augur rig.

Figure 12. Preparing to drive the casing.

Figure 13. Unloading the reinforcing cage.

Figure 14. Pouring the concrete.

Pile Testing

In order to observe the effect of cyclic axial loading on pile behaviour, it was necessary to compare the behaviour of piles that were subjected to cyclic axial loading with some piles which were not. For this reason, four of the piles were tested monotonically without any cyclic loading and the results from these tests were used as a "baseline" of pile uplift capacity and stiffness. The remaining five piles were subjected to a synthetic "earthquake" (30 cycles of reversing direction axial load) before also being loaded to failure in uplift.

For convenience, the four corner piles of the group were used for the monotonic load tests. Loads were applied by using a servo-hydraulic actuator mounted in a 7 m long steel truss. The truss was spanned across each corner pile diagonally, as shown in Figure 15, with the ends supported on heavy timber and concrete bearers laid on the ground. Details of the truss are shown in Figures 16 and 17.

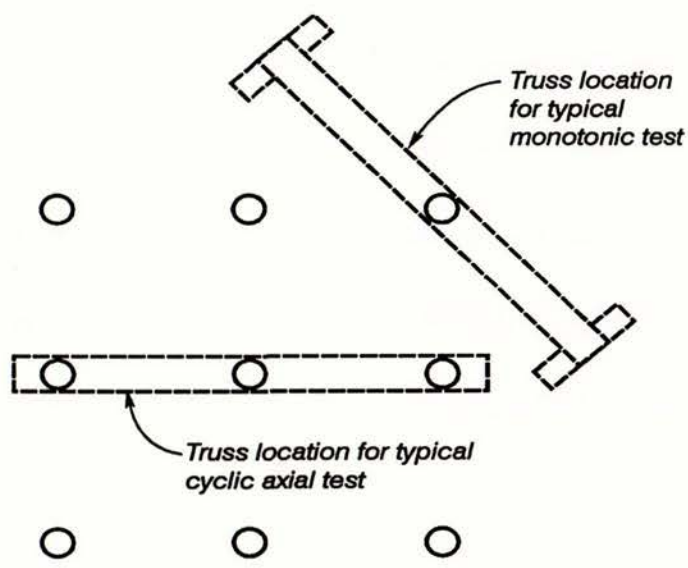

Figure 15. Truss layout for monotonic uplift and cyclic load tests.

Once the corner piles had been tested in this way, the remaining piles were tested by spanning the truss parallel to the grid and using the already-tested piles to provide the necessary up-and-down reaction forces, as shown in Figure 15. This arrangement allowed cyclic loads of reversing direction to be applied to each pile under test because the corner piles still had adequate capacity to provide the necessary anchorage in both compression and uplift.

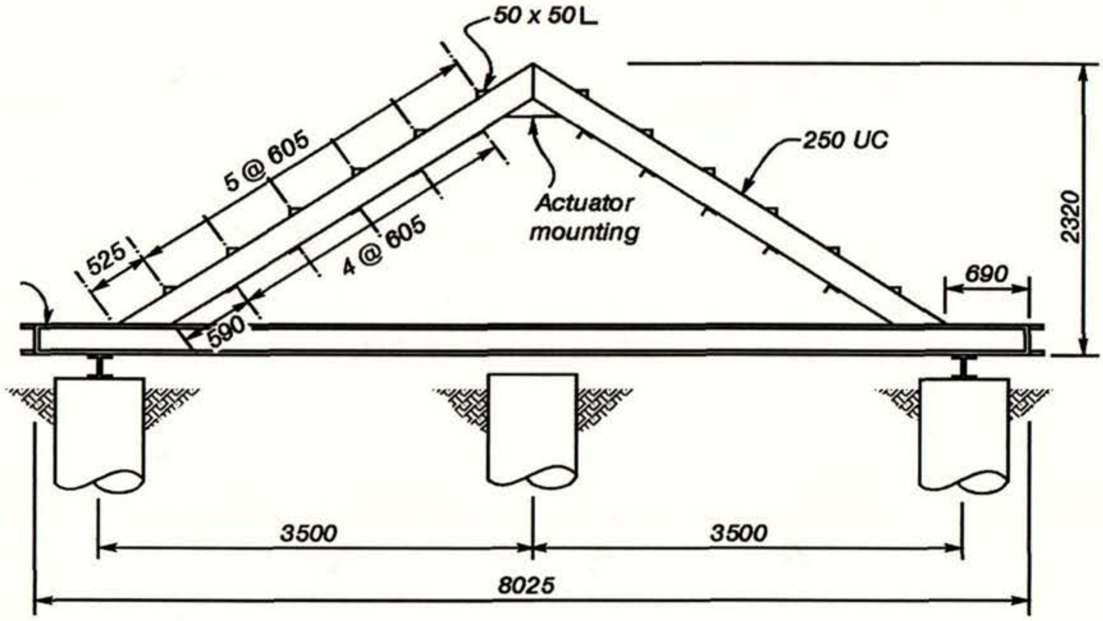

Figure 16. Loading truss details.

The servo-hydraulic actuator used was an MTS model 204.81 of 500 kN capacity and 152 mm stroke with an integral LVDT and an MTS model 72-233C servo-valve. A close-coupled load cell manufactured by the University of Canterbury, Department of Civil Engineering was used to measure load and heavy universal joints, also manufactured within the Department, were used at each end of the assembly to provide the necessary freedom from induced bending moments. Hydraulic power was provided by an MTS hydraulic power unit of 62 l/min capacity. Electrical power for this unit was provided by a 110 kVA mobile generator.

Figure 17. View of loading truss and actuator.

The load applied to the pile was controlled using an MTS model 443 test controller and an MTS model 413.05 master controller. The key components of the electro-hydraulic test system are shown schematically in Figure 18 with the servo control loop indicated. The low-level electrical output of the load cell is measured by the calibrated signal conditioner, and the sensed load is output as a ± 10 volt analogue signal. The desired load is input from the computer controlled signal generator to the test controller as a similar ± 10 volt analogue signal. The sensed load and the desired load are compared by a summing amplifier and the difference, or error signal, is output to the valve driver, which generates the necessary current to operate the servo-valve. The performance of the loop is optimised by varying the amplification, or gain, applied to the error signal.

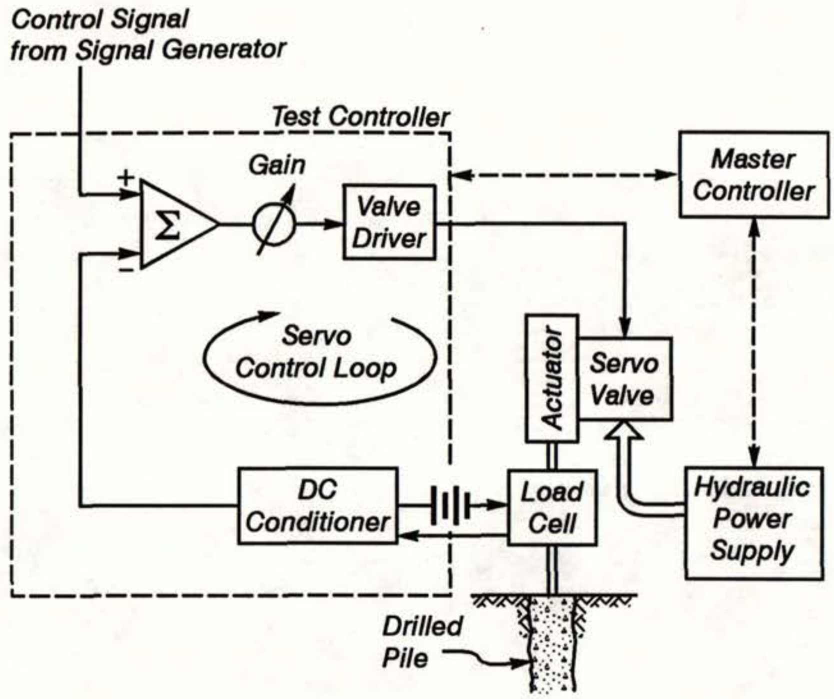

Figure 18. Servo control system.

Each test was run under the control of a personal computer as shown schematically in Figure 19. First, the required load history was generated interactively by the computer and downloaded to an HP33120A arbitrary waveform generator. Next the HP75000 data acquisition system, consisting of an E1351A 16 channel FET multiplexer and E1326B 5 1/2 digit multimeter, was initialised and configured to receive the data. Meanwhile, the hydraulic system was brought up to operating temperature by cycling the actuator up and down slowly. Next, the actuator was fastened to the pile head, the waveform generator triggered, and the servo-system commenced loading the pile. During the test, data was streamed into computer mass memory. On completion, data was converted to engineering units and stored onto hard disk, the oil pressure was released, and the actuator disconnected from the pile head.

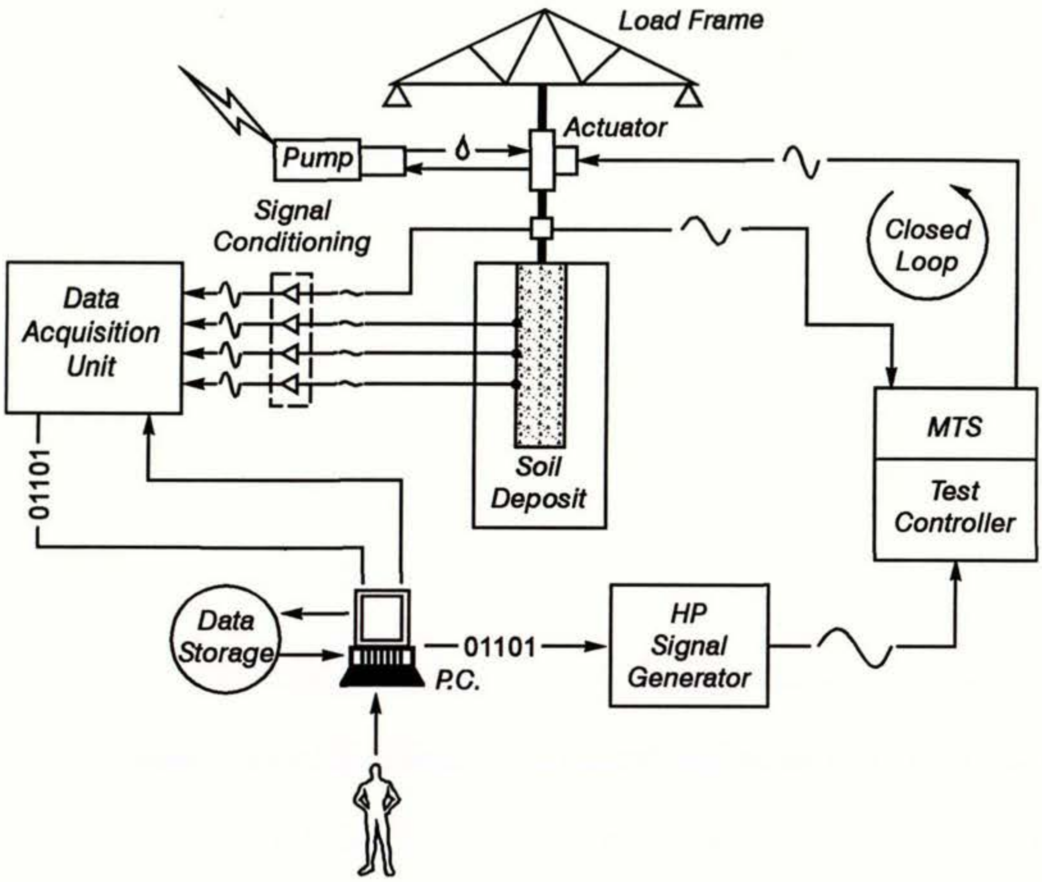

Figure 19. The overall load test system

Instrumentation consisted of load cell, pile displacement transducer, and three strain gauges attached to one of the longitudinal reinforcing bars. The load cell output was measured as a ± 10 volt analogue signal as output from the MTS signal conditioner. Pile displacement was measured by a LSCT transducer which was attached to a 5 m long aluminium surveying staff spanning perpendicular to the load frame and supported at each end by wooden blocks resting on the soil. This transducer was connected directly to the data acquisition system. The three strain gauges were each wired in a quarter bridge arrangement and connected to individual Measurements Group 2310 signal conditioners with a gain of 10,000 being used. Output from the signal conditioners was then connected to the data acquisition system.

The intended purpose of mounting strain gauges on the reinforcing cage was to try and measure the distribution of side resistance of the pile with depth.

All of the electronic control and data acquisition equipment was housed in a caravan for protection from the weather and also for security, with the caravan being removed from site at the end of each working day. The arrangement of equipment inside the caravan is shown in Figure 20.

Figure 20. Control room setup inside the caravan.

The MTS hydraulic pump was housed inside a standard shipping container, also for reasons of security and weather-tightness. The mobile generator was self contained with a weather-tight, lockable enclosure. An overall view of testing in progress on site is given in Figure 21.

Figure 21. Arrangement of equipment on site.

Pile Response

The results for all of the pile load tests are summarised in Table 4 and all of the load-displacement curves are given in Appendix A. The first test, EQC01, encountered significant difficulties with the test apparatus and may best be regarded as a "shakedown" of the equipment and test procedures. An electrical failure of the load cell occurred during test EQC08 and so this test had to be abandoned with no useful data being obtained. For test EQC03 some problems were encountered with settlement of the truss end supports and so the test was repeated as EQC03A.

Table 4. Bored pile load test data.

Test No.	Q_u (kN)	L_c (kN)	LRL	m	K_i (kN/m	K_f (kN/m	δ_{ppi} (mm)	δ_{ppf} (mm)	δ_p (mm)
EQC02	361	-	-	-	987	-	-	-	-
EQC03	458	-	-	-	768	-	-	-	-
EQC03A	444	-	-	-	450	-	-	-	-
EQC04	449	-	-	-	847	-	-	-	-
EQC05	453	257	0.61	1.07	192	93	4.8	7.6	-1.3
EQC06	423	337	0.80	1.00	306	19	1.8	5.9	-2.3
EQC07A	-	42	0.10	-	521	405	0.1	0.1	0.0
EQC07B	411	296	0.70	0.97	466	30	1.8	6.5	-2.1
EQC09A	-	100	0.24	-	459	463	0.4	0.4	-0.1
EQC09B	516	210	0.50	1.22	505	265	0.7	1.1	-1.2

Q_u	Maximum interpreted capacity
L_c	Half amplitude of cyclic load (nominal, computed for first load cycle)
LRL	Level of Repeated Load, L_c / average Q_u for monotonic tests
m	Uplift capacity change coefficient, Q_u / average Q_u for monotonic tests
K_i	Initial stiffness for first load cycle
K_f	Initial stiffness for final load cycle
δ_{ppi}	Peak-to-peak displacement for first load cycle
δ_{ppf}	Peak-to-peak displacement for final load cycle
δ_p	Permanent displacement after final load cycle

In order to increase the amount of data obtained from the limited number of piles available for testing, it was decided to apply two simulated earthquake load tests to bored piles EQC07 and 9. The first tests in each case (EQC07A and EQC09A) were of comparatively low level (LRL = 0.10 and 0.24) and were terminated prior to applying the monotonic uplift to failure sequence. The second tests (EQC07B and EQC09B) were at a much higher level of loading (LRL = 0.70 and 0.50) and the results of these were not expected to be much affected by the earlier low-level loading.

The load-displacement response for the monotonic uplift test EQC04 is shown in Figure 22 and is typical of the three monotonic uplift load tests from this study. The shape of the curve is typical of many other uplift load tests for bored piles reported in other studies [12], with three distinct regions being identified: initial linear, transition, and final linear, as shown schematically in Figure 23. For the final linear portion of the curve, creep displacements become significant and so the shape of this part of the curve depends on the rate of loading and the ability of the load system to keep pace with the creep rate. Consequently this part of the load-displacement curve is considered to be an unreliable indication of the true behaviour of the pile. Similarly, the maximum load measured during each test is considered to be an unreliable indication of the pile capacity. For this study, the maximum load recorded for each test was determined largely by the actuator capacity and hydraulic oil pressure which had to be increased during the test programme because the loads encountered were larger than expected.

For these reasons it is necessary to make some consistent interpretation of capacity from the pile load-displacement curves. Many different methods have been suggested and a recent study by Hirany and Kulhawy [12] has analysed the strengths and weaknesses of them. The methods proposed range from complex graphical methods [e.g. 13] to simple procedures such as stating the load at a standard displacement [e.g. 14]. For this study, the "uplift slope tangent method" [15, 16] was found to be the most useful and so has been used to interpret the results for all of the tests terminating in uplift to failure. Application of the method is illustrated in Figure 24.

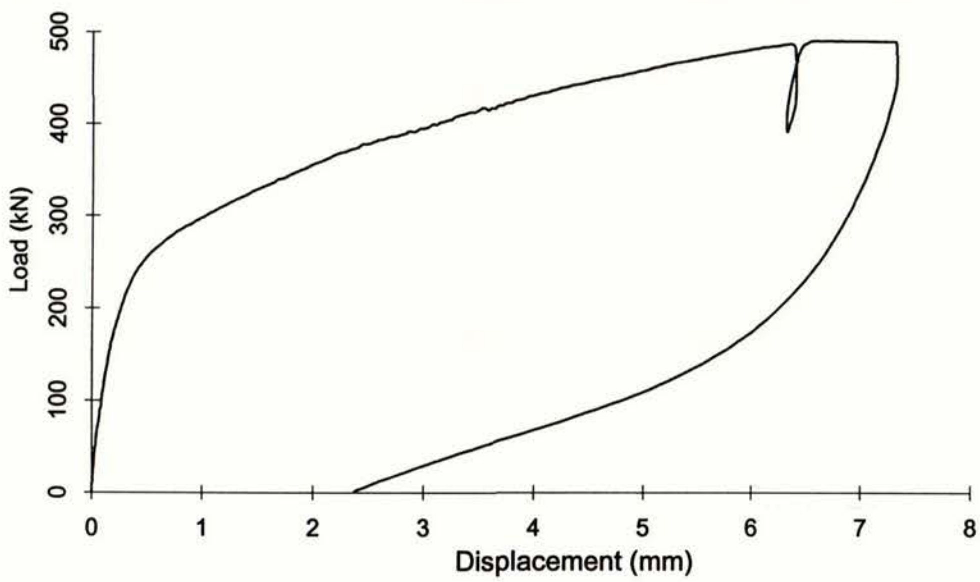

Figure 22. Load versus displacement for monotonic uplift load test EQC04

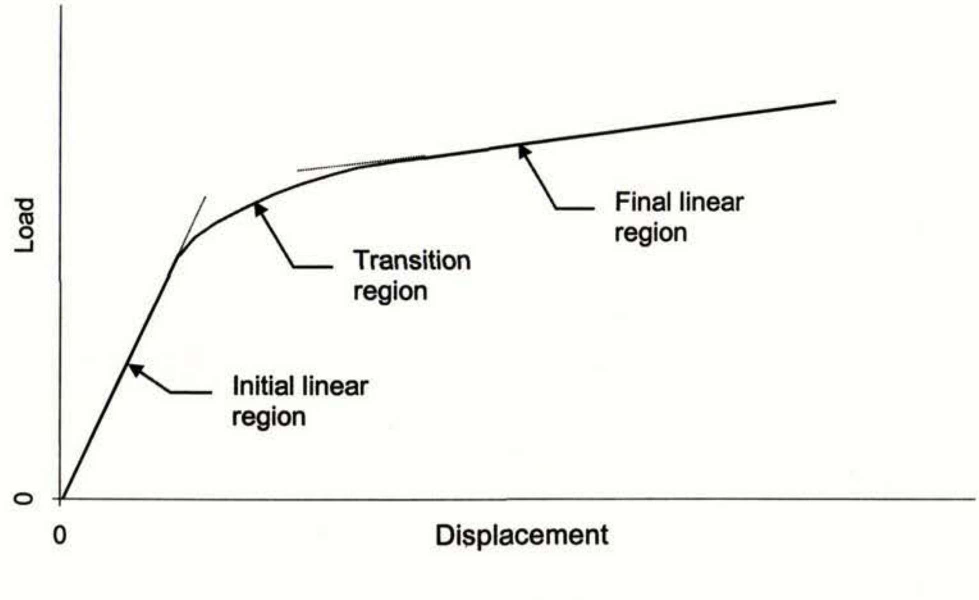

Figure 23. Regions of load-displacement curve.

Source: Hirany and Kulhawy [12]

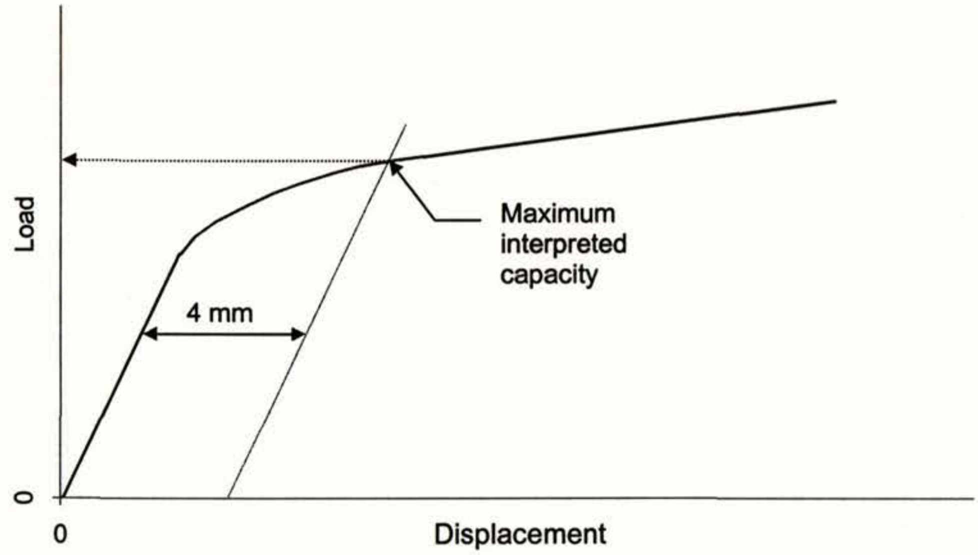

Figure 24. Uplift slope tangent method.
Source: Hirany and Kulhawy [12]

The maximum interpreted capacity (Q_u) for each of the monotonic uplift load tests without earthquake loading (EQC02, 3, and 4) is given in Table 4. The average value of Q_u for these three tests is 423 kN which has been taken as a "baseline" value of pile capacity for computing the values of LRL and *m* shown in Table 4.

All of the other piles (EQC05 to 9) were subjected to different levels of simulated earthquake loading prior to being loaded to failure in uplift. The level of repeated loading (LRL) applied in each case was varied systematically from 0.10 (EQC07A) to 0.70 (EQC07B) while all other loading variables were kept as constant as possible. Some difficulty was experienced during load test EQC06 because the load cell zero point drifted during the test. This drift combined with a drop of hydraulic oil pressure as the pile "softened" under the high cyclic loading caused a drop in cyclic uplift load during the test. A similar problem occurred during load test EQC07B. The load cell failed completely during load test EQC08. However, despite these technical difficulties the trends of pile response have been adequately demonstrated.

At low values of LRL (LRL = 0.10, 0.24), the pile response was largely elastic, as illustrated in Figure 25, with no significant degradation in stiffness or permanent displacement. By contrast, at high values of LRL (LRL = 0.61, 0.70, 0.80), the pile response was highly inelastic, as illustrated in Figure 26, with degradation in stiffness with each cycle of loading and narrowing of the hysteresis loops which contain "slop" between the compression and uplift cycles. None of the piles pulled out of the ground and all nominally maintained their pre-earthquake capacity ($m = 0.97$ to 1.22), however, interpretation of maximum capacity was difficult in those cases where severe degradation in stiffness occurred. The most deleterious features of the response observed were dramatic reduction in initial stiffness (by a factor of up to 16.1), large increase in peak-to-peak displacement, and the thin, sloppy shape of the load-displacement hysteresis curves.

Load test EQC09B represents an intermediate case between the observed response of low and high values of LRL (LRL = 0.50), with the load -displacement response shown in Figure 27. Some degradation in stiffness occurred (K decreased by a factor of 1.9) but the hysteresis loops remained elliptical in shape.

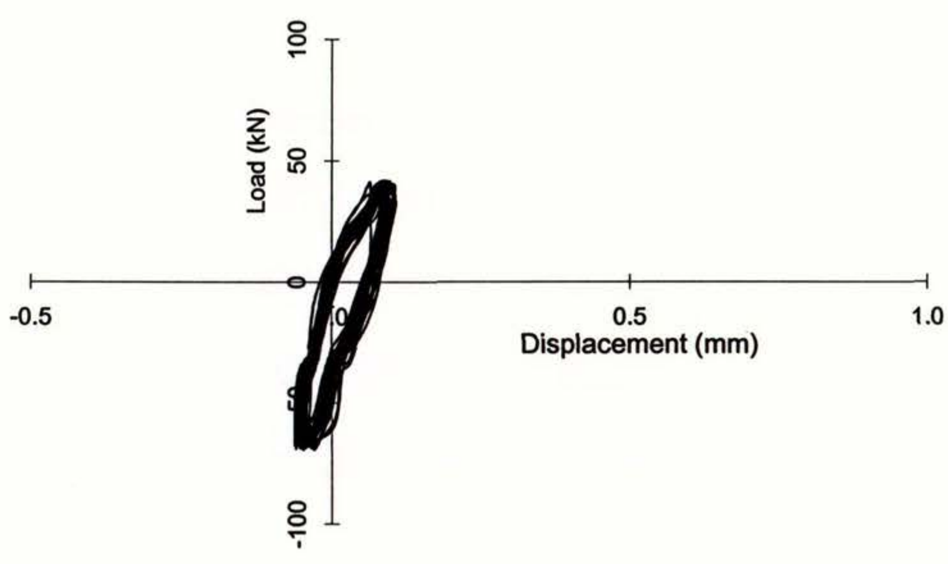

Figure 25. Load versus displacement for test EQC07A (LRL = 0.10)

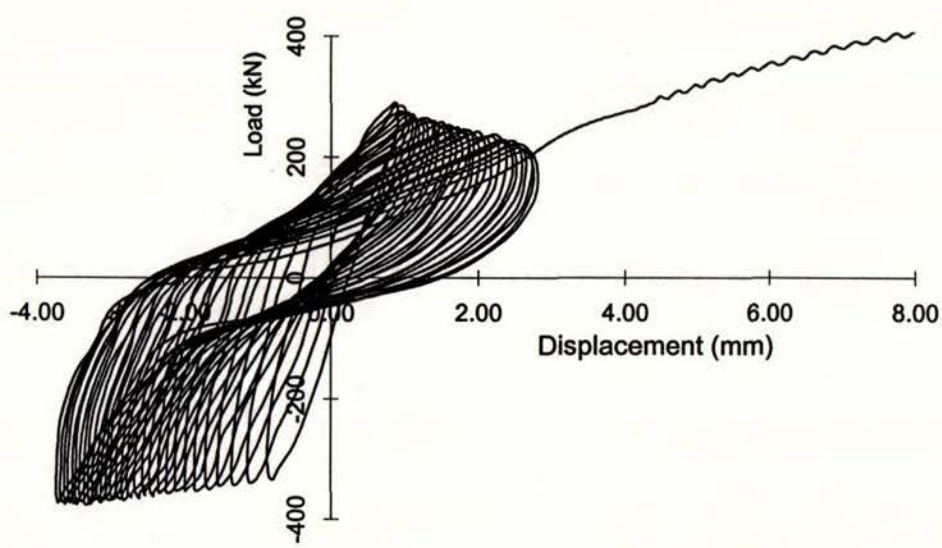

Figure 26. Load versus displacement for test EQC07B (LRL = 0.70)

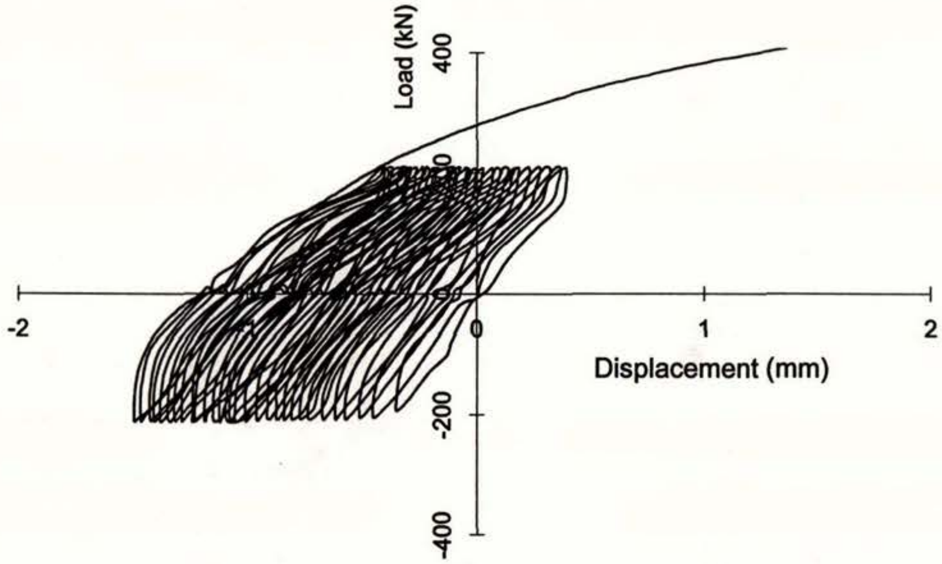

Figure 27. Load versus displacement for test EQC09B (LRL = 0.50)

Model—Prototype Comparison

The primary objective of this project was to test the predictions from existing model studies in laboratory prepared soil deposits for full-size prototype piles. In particular, the recent study of McManus and Chambers [10] was selected as being the most relevant of those available because it simulated earthquake conditions specifically. Most other studies have simulated wind or wave loading conditions which involve long sequences of low frequency loading compared with earthquake conditions which involve short sequences of high frequency loading.

Whenever cyclic loading on piles is being considered, an enormous range of variables becomes apparent: Frequency, waveform, duration, amplitude, and mean load. Also, a pile may be subjected to simultaneous lateral and moment loading each with a similar list of possible variables. For any meaningful progress to be made in the understanding of pile behaviour it is necessary, within any particular study, to freeze as many of these variables as possible while focusing on the effects of one or two of them. The model study of McManus and Chambers examined axial loading without any lateral or moment loading and fixed the frequency, waveform, and duration at representative values (1 Hz, sine wave, 30 cycles). The amplitude of cyclic loading and the mean load both were varied systematically to fill out the cyclic stability diagram shown in Figure 4. A total of 25 models were tested.

For this full-size study, it was not considered feasible to repeat all 25 of the model tests. Instead, it was decided to focus on the most critical area of the cyclic stability diagram from the model study, which was the central axis of the diagram where mean load is zero. A total of six full-size cyclic load tests were performed, all with zero mean load.

The physical attributes of the full-size pile tests also were made to match the model study as closely as practicable given the great differences in scale. The piles were built above the water table although the soil was, inevitably, damp. The soil was granular but, unlike the model deposits of clean sand, contained a certain amount of fines. The construction processes used were very similar, both model and full-size piles were constructed using a steel casing which was withdrawn during concrete pouring, the only difference being that the full-size casing was driven while the model casing was placed prior to depositing the soil around it. The main physical difference between model and prototype piles was their length/diameter (L/D) ratios, 15.3 for the model but only 7.3 for the prototype. This compromise was necessary for several reasons: a desire to make the prototype piles as large as possible, the availability of casing and augers, and the inability to loosen the site soil to a greater depth.

The most obvious difference in response between model and prototype is that none of the full-size piles pulled out during the tests even though significant deleterious behaviour was observed. The response of the comparable model tests was much more clear cut, with those piles showing unstable behaviour pulling out of the soil. Two of the full-size pile tests (EQC06 and 7B) showed instability as evidenced by: (a) large decrease in stiffness (by a factor of up to 16), (b) continually decreasing stiffness, and (c) continual cycle-by-cycle increase in uplift displacement. A third test (EQC05) was considered borderline unstable as it showed all three of these symptoms but at a much lower level. Identification of the unstable pile response is made in Table 5 and the results are shown plotted on a cyclic stability diagram in Figure 28.

There are at least two possible reasons why these unstable full-size piles did not fail completely by pullout. It is evident (e.g. Figure 26) that the hydraulic loading system was unable to maintain the full cyclic load as these piles softened because of oil flow rate limitations. Real earthquake loading is not likely to be so forgiving although the pile softening may be viewed, perhaps, as a crude form of base isolation. There may also be inertial effects to consider because of the great difference in mass between the model and prototype (by a factor of 200) while the same frequency of loading (1 Hz) was maintained for both tests.

Table 5. Cyclic load test summary.

Test No.	LRL	K_i/K_f	$\delta_{ppf}/\delta_{ppi}$	δ_u (mm)	Rating[a]
EQC07A	0.10	1.3	1.0	+0.1	S
EQC09A	0.24	1.0	1.0	+0.1	S
EQC09B	0.50	1.9	1.6	-0.4	S
EQC05	0.61	2.1	1.6	+1.2	S/U
EQC07B	0.70	15.5	3.6	+2.7	U
EQC06	0.80	16.1	3.3	+2.6	U

LRL Level of repeated load

K_i/K_f Ratio of initial stiffness of first and final load cycles

$\delta_{ppf}/\delta_{ppi}$ Ratio of peak-to-peak displacement for first and final load cycles

δ_u Pile displacement at peak of final uplift load cycle

a S = stable, U = unstable

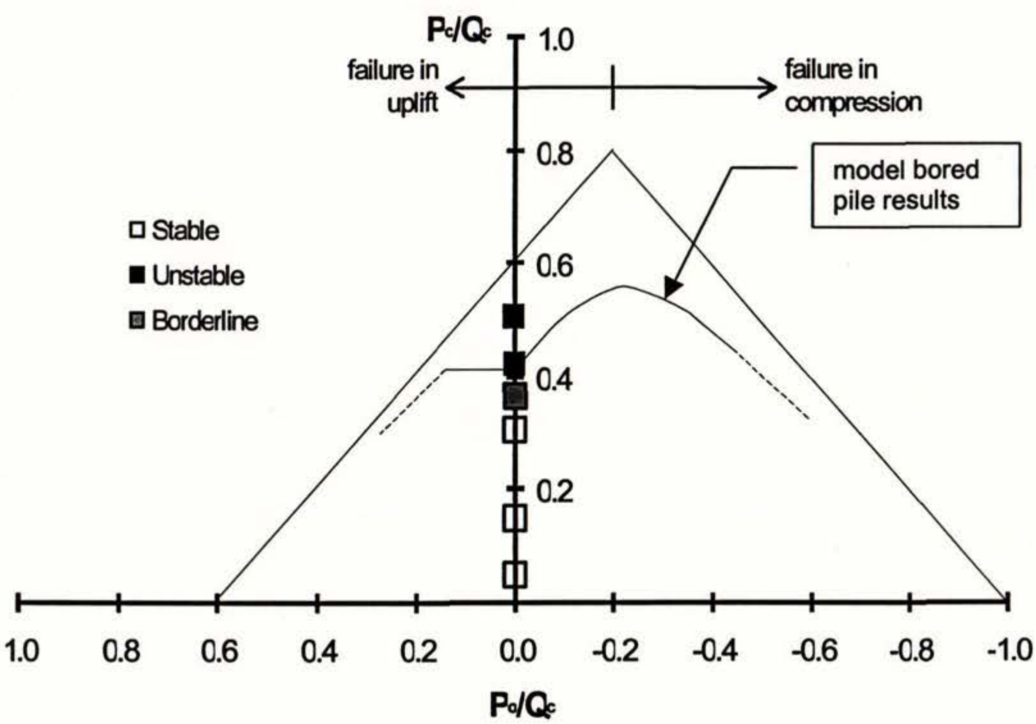

Figure 28. Cyclic stability diagram for full-size bored piles.

From Table 5, the value for the critical level of repeated loading (CLRL) for the full-size pile load tests was determined to be approximately 0.6. This value compares with a value of 0.67 for the model study of McManus and Chambers [10] and a range of 0.24 - 0.47 for piles with a L/D ratio of 8 in loose sand from the study of Turner and Kulhawy [6]. The difference with the latter study can be explained by the much greater number of cycles applied in that case (100 compared with 30 for this present study). The difference with the former model study can not be so easily explained and may be attributable to the large difference in scale between the model and prototype piles (scale factor $\approx$ 8 on pile diameter). The differences in soil properties between the two studies may also be a factor.

The difference between values for CLRL of 0.6 and 0.67 for prototype and model are not of great significance when compared with the variation reported for CLRL with different pile geometries and soil conditions. Trends for CLRL as a function of soil condition and pile geometry are given in Table 1 with a range of from 0.65 to 0.08. Generally, model studies have shown that CLRL increases with decreasing L/D ratio (piles becoming more squat) and decreases with increasing soil density. Therefore, the difference in CLRL between the prototype and model may be caused by differences in soil density, with the sand used in the model study being particularly loose (I_d = 14 % for the model, I_d = 20 % for the prototype).

In summary, the full-size load tests have demonstrated that significant degradation in pile response occurs at the same level of repeated load (more or less) as for a model study programme carried out under similar conditions. The switch from "good" pile response at one load level to "bad" response at another, higher, load level occurred quite abruptly, also as demonstrated previously by model studies. One significant difference between model pile behaviour and full-size pile behaviour was the reluctance of the full-size piles to pull out of the soil. This may be a shortcoming of the hydraulic loading system but may also be a feature of the large increase in scale.

Recommendations for Practice

The results of these full-size bored pile load tests have confirmed the predictions of earlier model studies that significant degradation in pile behaviour is caused by cyclic axial loading at modest levels. For this study, only one soil condition (loose, granular) and one pile geometry (L/D = 7.3) were investigated but it is possible to extrapolate the results to other soil conditions and pile geometries by using the trends reported for other, relevant model studies. In Table 6, the result of this study has been combined with the trends from the study of Turner and Kulhawy [6], given in Table 1, to make recommendations for CLRL, albeit in a simple minded way: The values in Table 1 have been averaged, rounded to one decimal place, and 0.2 added to account for the apparent difference in outcome caused by the larger number of cycles in that study (100 cycles compared with 30).

Table 6. Critical level of repeated load for bored piles in granular soil.
(N = 30, f = 1 Hz)

Soil condition	CLRL D/B=4	CLRL D/B=8
Loose	0.8	0.6
Medium	0.5	0.4
Dense	0.5	0.3

For piles in cohesive soil, no firm recommendation can be made. However, results from the model study of McManus and Kulhawy [7] in silt-clay indicate that similar values to those above may be expected if the usual equivalence is made between loose condition for granular soil and normally consolidated condition for cohesive soil and between dense granular soil and over-consolidated cohesive soil.

For more slender piles (L/D > 8), again, no firm recommendation can be made. Prudence suggests that the values of CLRL given for L/D = 8 be adopted pending further investigation.

Given the substantial degradation in performance observed for those piles in this study which were loaded to levels greater than the CLRL, it would be prudent for designers to limit cyclic axial loads to below the CLRL during an earthquake. For the case where zero mean load is applied to the pile during an earthquake, the applied cyclic load should be limited by:

$$P_c < CLRL \times Q_t \qquad (1)$$

in which P_c = applied cyclic load amplitude and Q_t = pile uplift capacity.

Usually, a mean axial load will be applied to the pile during an earthquake from structural dead and live loads, simultaneous with any cyclic axial loads. The interaction between mean and cyclic loads was not investigated in this study. However, guidance is available from the study of McManus and Chambers [10] which considered mean loads both in uplift and compression, as summarised by the cyclic stability diagram shown in Figure 4. The recommendations from the study have been adapted as follows: For the case of mean load in uplift, the cyclic load should be limited by:

$$P_c < CLRL \times Q_t, \qquad P_c + P_0 < Q_t \qquad (2)$$

in which P_0 = applied mean load.

For the case of low mean load in compression, the cyclic load should be by:

$$P_c < CLRL \times Q_t + |P_0|, \qquad |P_0| < \frac{|Q_c| - |Q_t|}{2} \qquad (3)$$

in which Q_c = pile compression capacity. For greater mean loads in compression, the failure mode changes from failure in uplift to failure in compression (see Figure 3). No results are available from this study concerning failure in compression, but, from the study of McManus and Chambers compression failure was found to be characterised by excessive settlement of the pile and a recommendation was made to limit cyclic axial load by:

$$P_c < 0.7 \times (Q_c - |P_0|), \qquad |P_0| > \frac{|Q_c| - |Q_t|}{2} \qquad (4)$$

In certain circumstances, designers may wish to exceed these recommended limits for cyclic axial load, allowing the pile stiffness to degrade and, effectively, a crude rocking motion to develop in the structure. Two warnings must be made concerning such a procedure: First, the fact that none of the test piles in this study pulled out of the ground does not mean that pullout may not occur during a real earthquake. The hydraulic load system was very kind to the test piles in this regard by dropping load as pile movements increased. Complete pullout of piles has been observed during actual earthquakes (e.g. see Figure 2). Second, differential pile settlement may be more of a problem during an actual earthquake than observed for the test piles in this study. The soil at the test site was loosened to a depth of only 6 m, or about one pile diameter beneath the tip of the piles. Below this depth was very dense gravel which might have hidden the tendency for pile settlement observed for the equivalent model study.

The effect on present pile design practice of these recommendations is uncertain because the present treatment of earthquake induced axial loads by designers is uncertain. Large factors of safety routinely are applied to gravity induced dead and live loads when designing bored piles (usually FS = 2.5), but what factor of safety designers presently apply to gravity plus earthquake load combinations is unknown and probably not uniform from one designer to another. The interplay of pile behaviour, loading, uncertainty, and risk inherent in the choice of factor of safety should be the subject of further investigation.

Summary and Conclusions

There is a growing amount of evidence that cyclic axial loading of pile foundations causes degradation in pile behaviour for all but the very lowest levels of repeated loading. Much of this evidence comes from laboratory scale model studies which are often viewed with skepticism, because of the difficulty in applying the laws of similitude to model test results in geomechanics. This study has confirmed, by testing full-size bored piles in the field, that significant degradation in pile behaviour does occur when cyclic axial loads representative of earthquake conditions are applied. Further, the level of repeated loading required to cause such degradation was found to be in general agreement with that predicted by an equivalent study carried out at model scale in the laboratory.

This confirmation of the model study outcome is significant because it allows the existing data from model studies to be applied to practice with more confidence. It will also encourage the planning of additional model studies to increase the amount of available data with far greater economy than is possible with full-size field studies. As a first step in this process, the results from this study have been combined with the results from a recent model study to provide recommendations to designers for limiting the level of cyclic axial load to be applied to bored piles during earthquakes. A limited range of load combinations, soil conditions, and pile geometries only was able to be considered. Further studies are needed to extend this range to cover all design situations.

The effect on present pile design practice of the recommendations contained herein is uncertain because the present treatment of earthquake induced axial loads by designers is uncertain. Large factors of safety routinely are applied to gravity induced dead and live loads when designing bored piles, but what factor of safety designers presently apply to gravity plus earthquake load combinations is unknown and probably not uniform from one designer to another. The interplay of pile behaviour, loading, uncertainty, and risk inherent in the choice of factor of safety should be the subject of further investigation.

References

1. Pender, M.J. (1993). "Aseismic pile foundation design analysis," Bulletin N.Z. National Soc. Earthquake Eng, Vol. 26, No. 1, pp. 49-160.

2. Girault, P. (1986). " Analyses of foundation failures," Proc. Int. Conf. The Mexico City Earthquakes - 1985, ASCE, pp 178-192.

3. Mendoza, M. J. and Auvinet, G. (1988). "The Mexico earthquake of September 19, 1985 - behavior of building foundations in Mexico City," Earthquake Spectra, Vol. 4, No.4, EERI, pp. 835-853.

4. Zeevaert, L. (1991). "Seismosoil dynamics of foundations in Mexico City earthquake, September 19, 1985," Journal of the N.Z. Society for Earthquake Engineering, Vol. 26, No.1, pp. 49-160.

5. Charlie, W. A., Turner, J. P., and Kulhawy, F. H. (1985). "Review of repeated axial load tests on deep foundations," Drilled Piers and Caissons II, Ed. C. N. Baker, Jr. ASCE, New York, pp. 129-150.

6. Turner, J. P. and Kulhawy, F. H. (1990). "Drained uplift capacity of drilled shafts under repeated axial loading," Journal of Geotechnical Engineering, ASCE, Vol.116, No.3, pp. 470-491.

7. McManus, K.J. and Kulhawy, F.H. (1994). "Cyclic Axial Loading of Drilled Shaft Foundations in Cohesive Soil," Journal of Geotechnical Engineering, ASCE, Vol 120, No. 9, Sep. 1994, pp. 1481-1497.

8. Poulos, H. G., (1988). "Cyclic stability diagram for axially loaded piles," Journal of Geotechnical Engineering, ASCE, Vol.114, No.8, Aug. 1988, pp. 877-895.

9. McManus, K.J. and Turner, J.P. (1996). "Axial capacity of bored pile foundations during earthquake loading," IPENZ Transactions Civil Section, Vol. 23, No. 1/CE, Nov. 1996, pp. 26-32.

10. McManus, K.J. and Chambers, A. (1995). "Stability Of Drilled Shafts Under Earthquake Induced Axial Loads," Performance of Deep Foundations Under Seismic Loading, Ed. J. P. Turner, ASCE Geotechnical Special Publication No. 51, p. 1-16.

11. Scott, R.F. (1979). "Laterally-loaded pile tests in a centrifuge," Centrifugal Modeling of Geotechnical Problems, Preprint 3786, ASCE National Convention, Atlanta.

12. Hirany, A and Kulhawy, F.H. (1988). "Conduct and interpretation of load tests on drilled shaft foundations," Report EL-5915, Electric Power Research Institute, Palo Alto, California.

13. Mansur, C.I. and Kaufman, J.M. (1956). "Pile tests, low-sill structure, Old River, Louisiana," J. of the Soil Mechanics and Foundation Division, ASCE, Vol. 82, No. SM5, pp. 1079/1-1079/33.

14. Terzaghi, K. And Peck, R.B. (1967). "Soil Mechanics in Engineering Practice, 2nd. Ed., John Wiley and Sons, New York, 533 p.

15. Kulhawy, F.H., Trautmann, C.H., Beech, J.F., O'Rourke, T.D., McGuire, W., Wood, W.A., and Capano, C. (1983). "Transmission line structure foundations for uplift/compression loading," Report EL-2870, Electric Power Research Institute, Palo Alto, California, 412 p.

16. O'Rourke, T.D. and Kulhawy, F.H. (1985). "Observations on load tests on drilled shafts," Drilled Piers and Caissons II, Ed. C.N. Baker, ASCE, New York, pp. 113-128.

Appendix A: Load test data

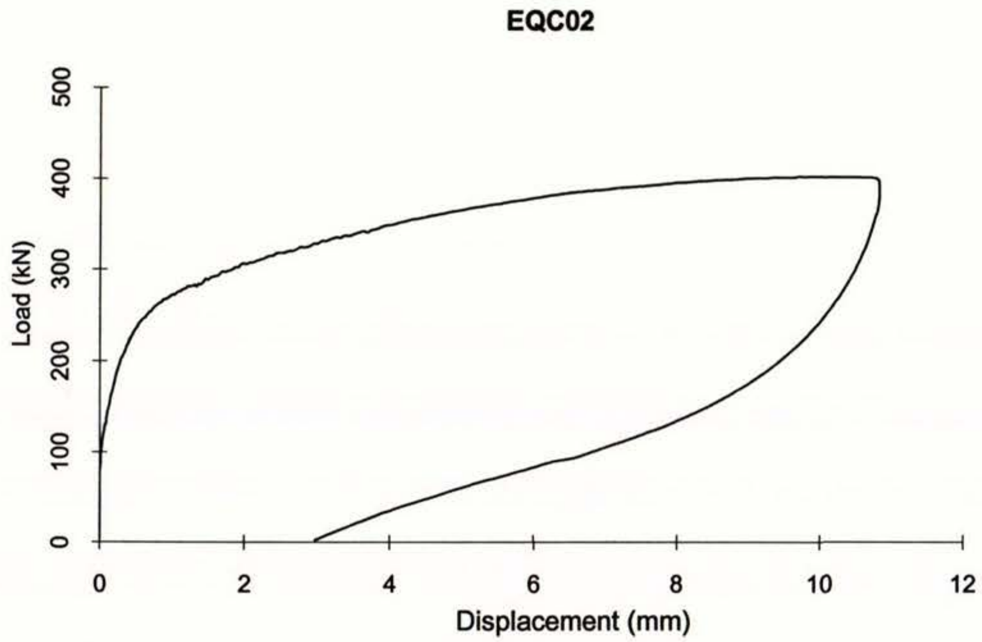

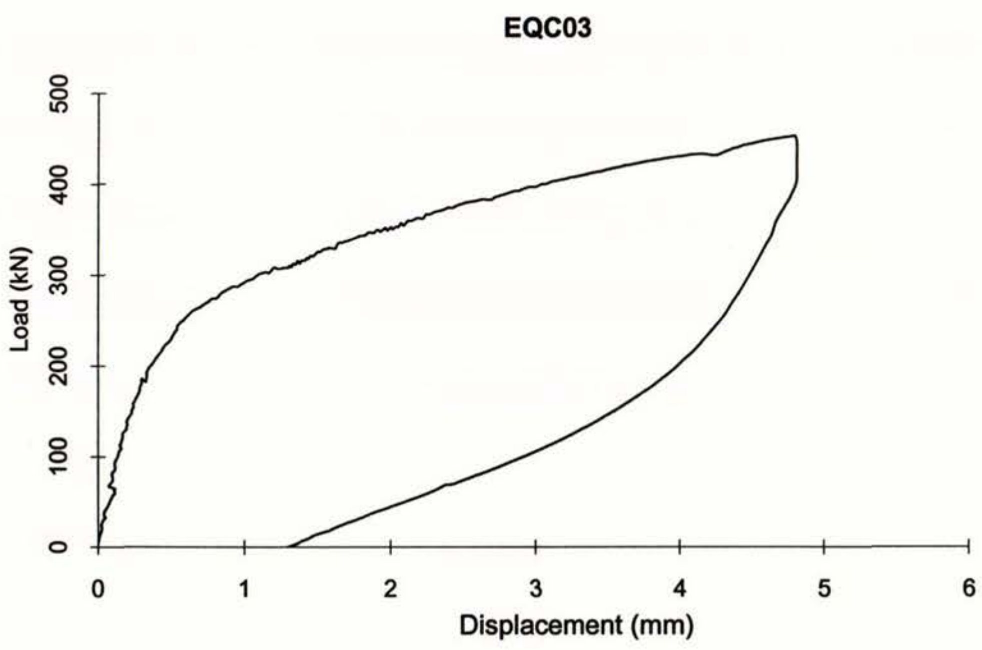

EQC03a

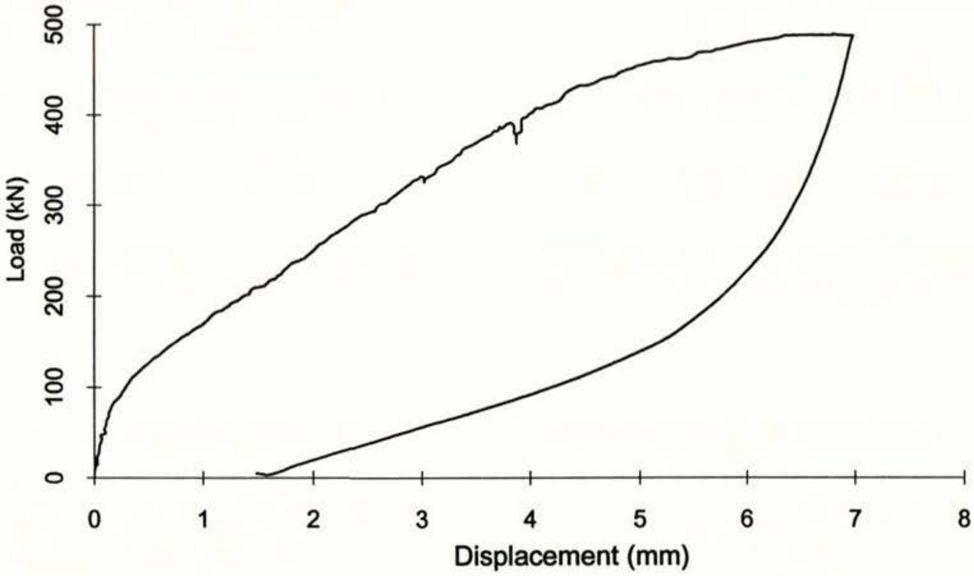

EQC04

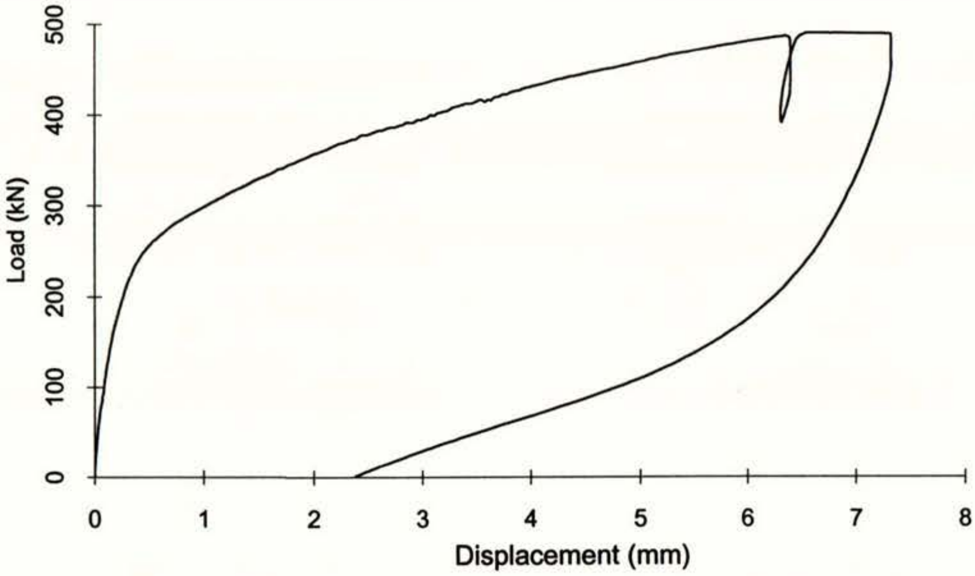

EQC05

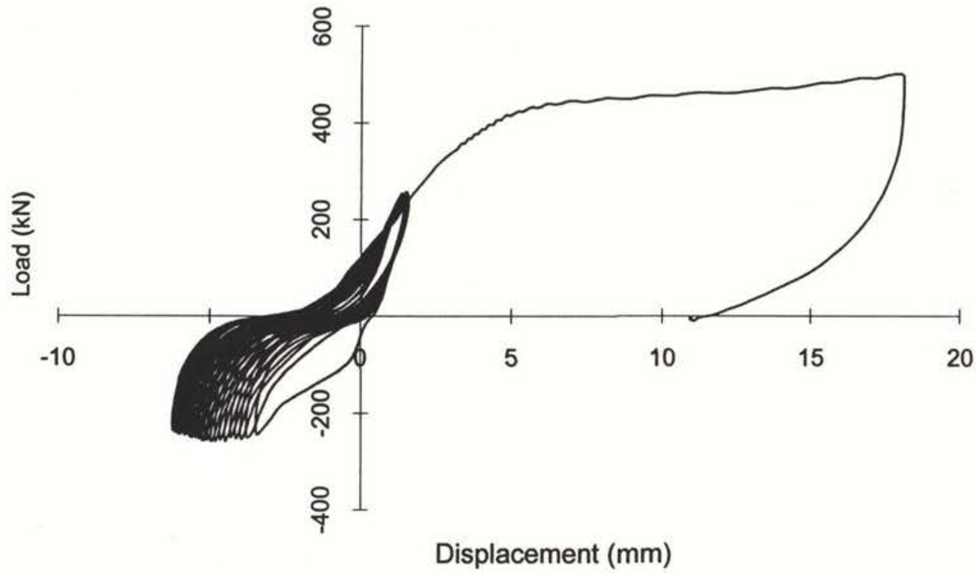

600
400
200
-200
-400
-10
0
5
10
15
20
Load (kN)
Displacement (mm)

EQC06

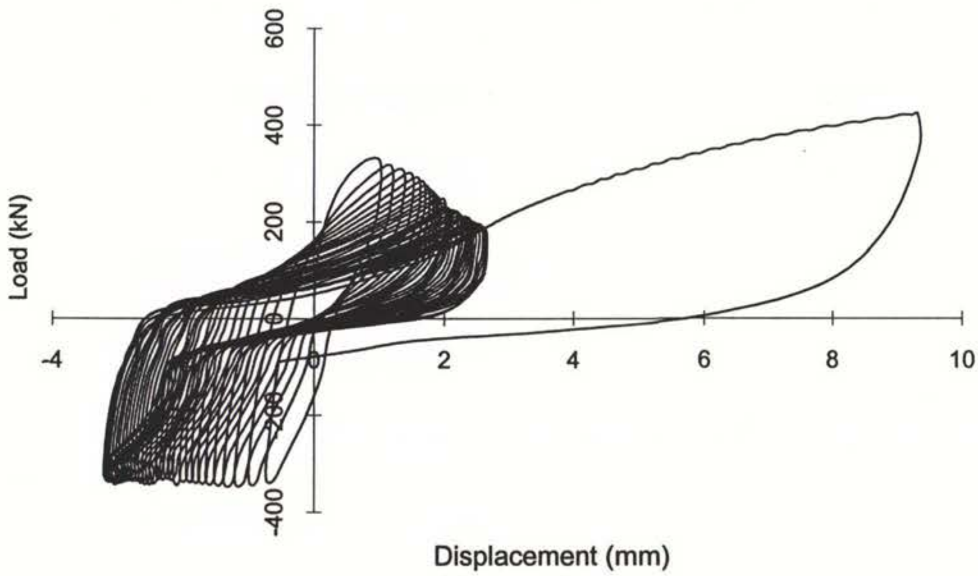

600
400
200
-200
-400
-4
0
2
4
6
8
10
Load (kN)
Displacement (mm)

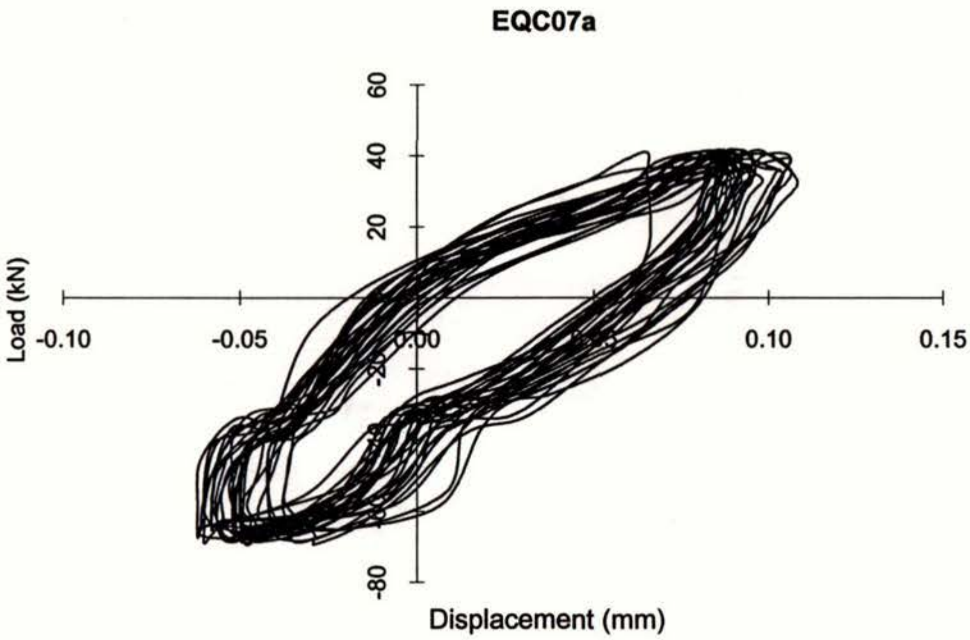
EQC07a
60
40
20
-20
-80
Load (kN)
-0.10
-0.05
0.00
0.10
0.15
Displacement (mm)

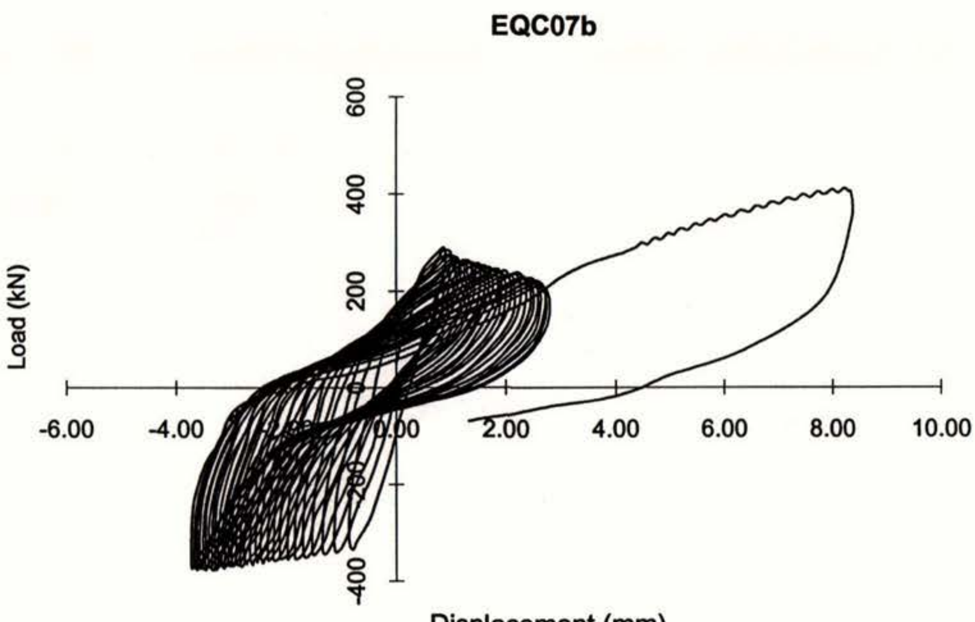
EQC07b
600
400
200
-400
Load (kN)
-6.00
-4.00
0.00
2.00
4.00
6.00
8.00
10.00
Displacement (mm)

EQC09a

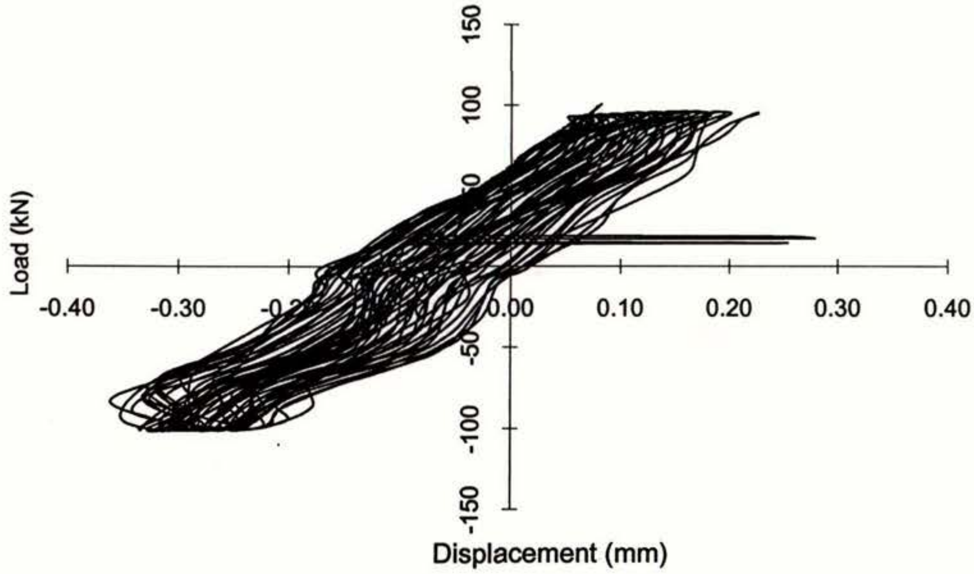

EQC09b

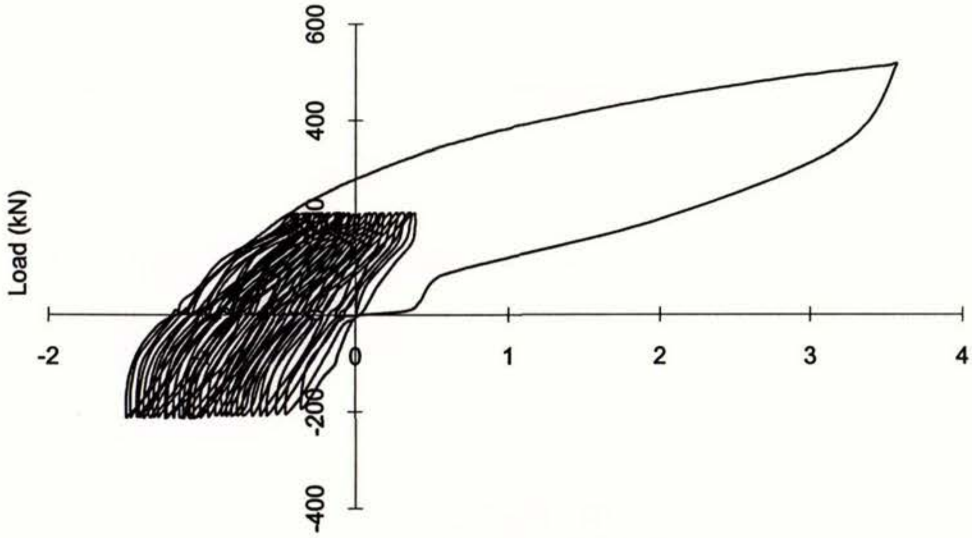

Appendix B: CPT test data

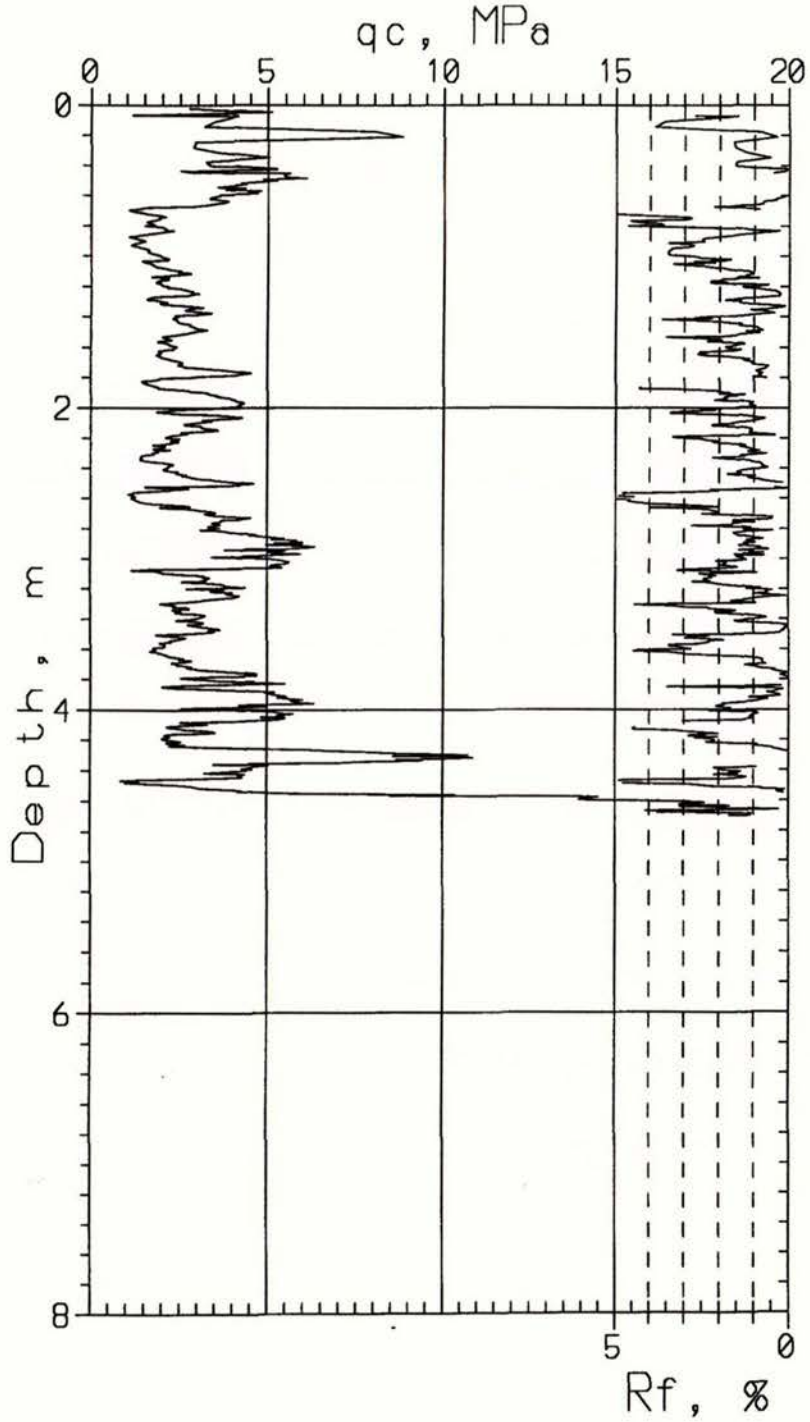

CPT test TEM001 29 February 1996

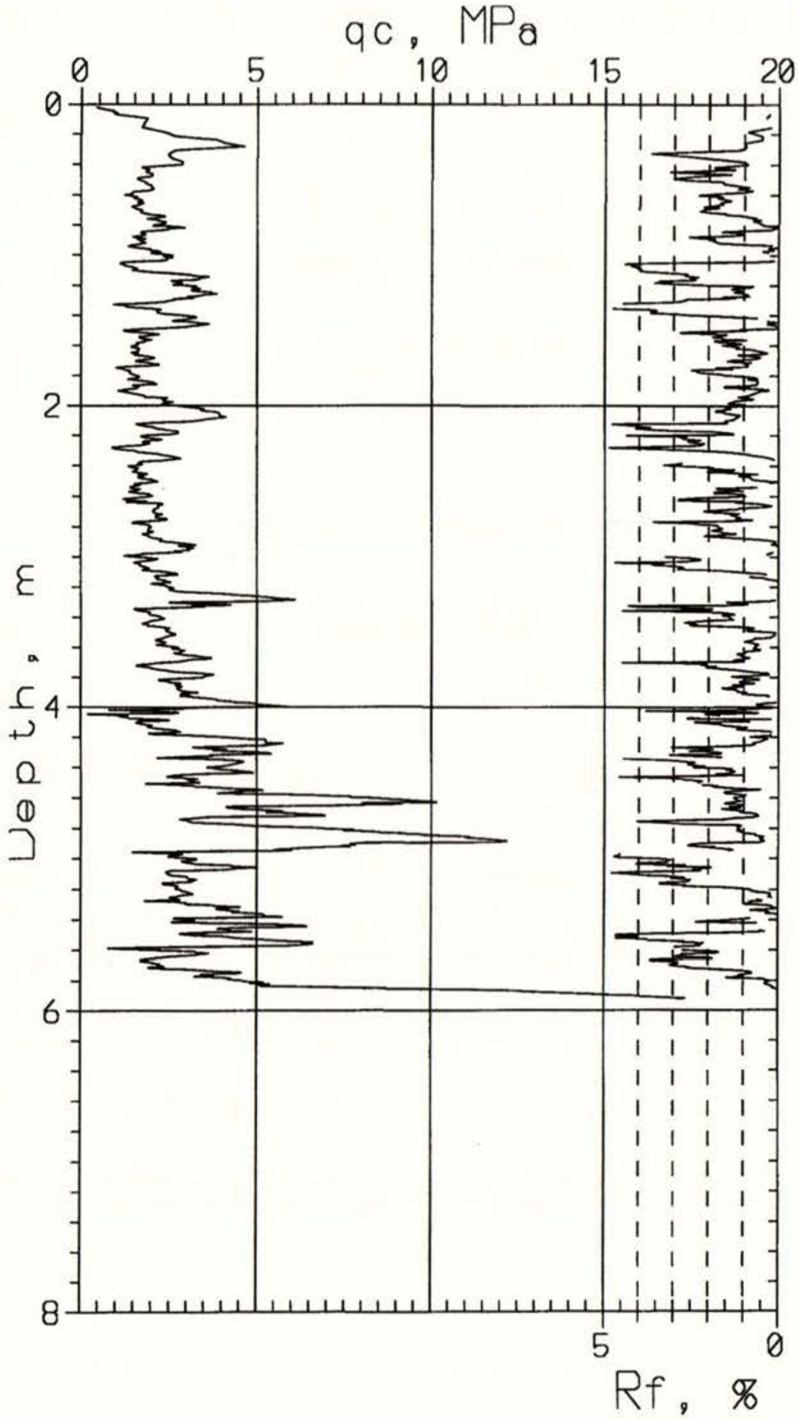

CPT test TEM002 29 February 1996

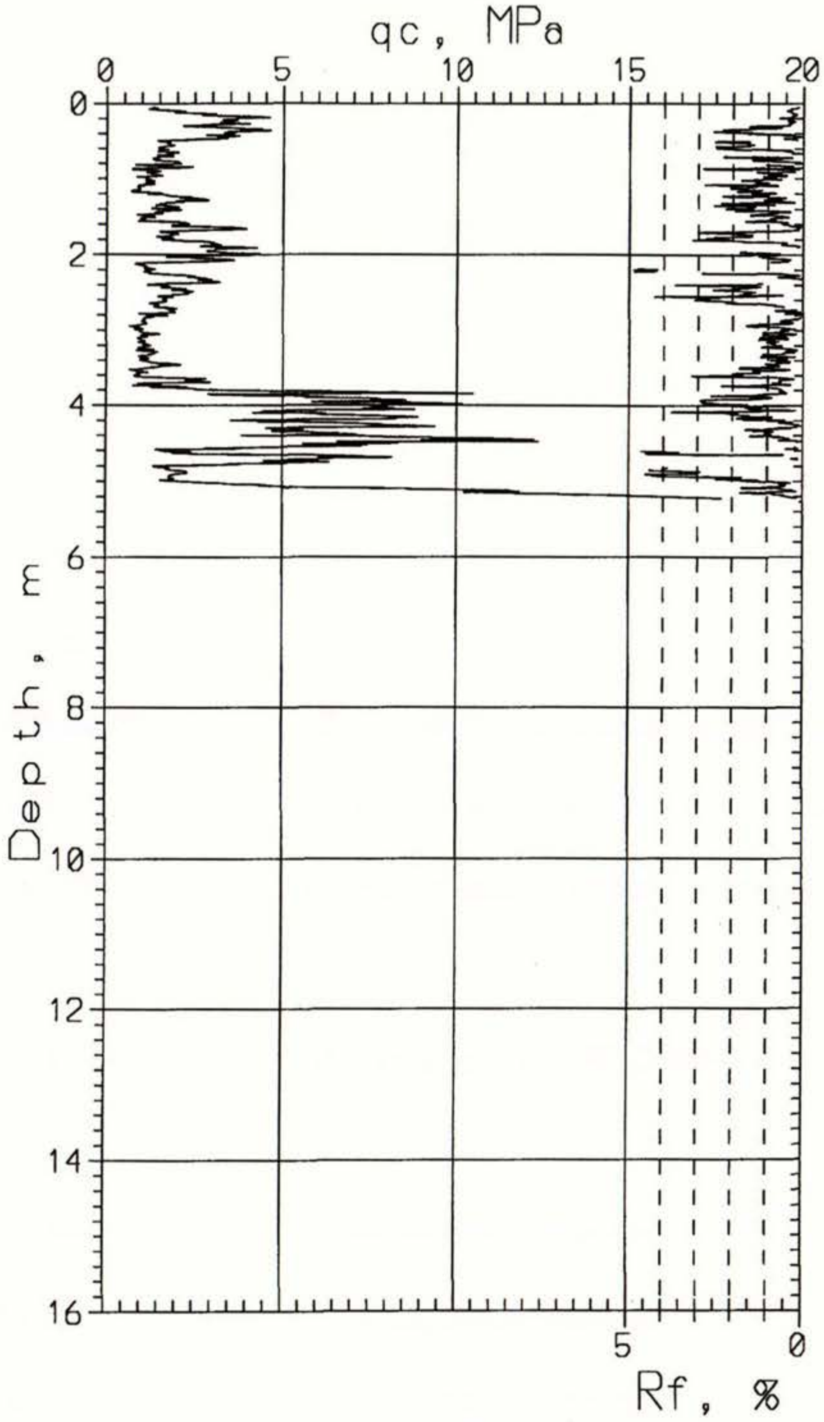

CPT test TEM004 28 May 1996

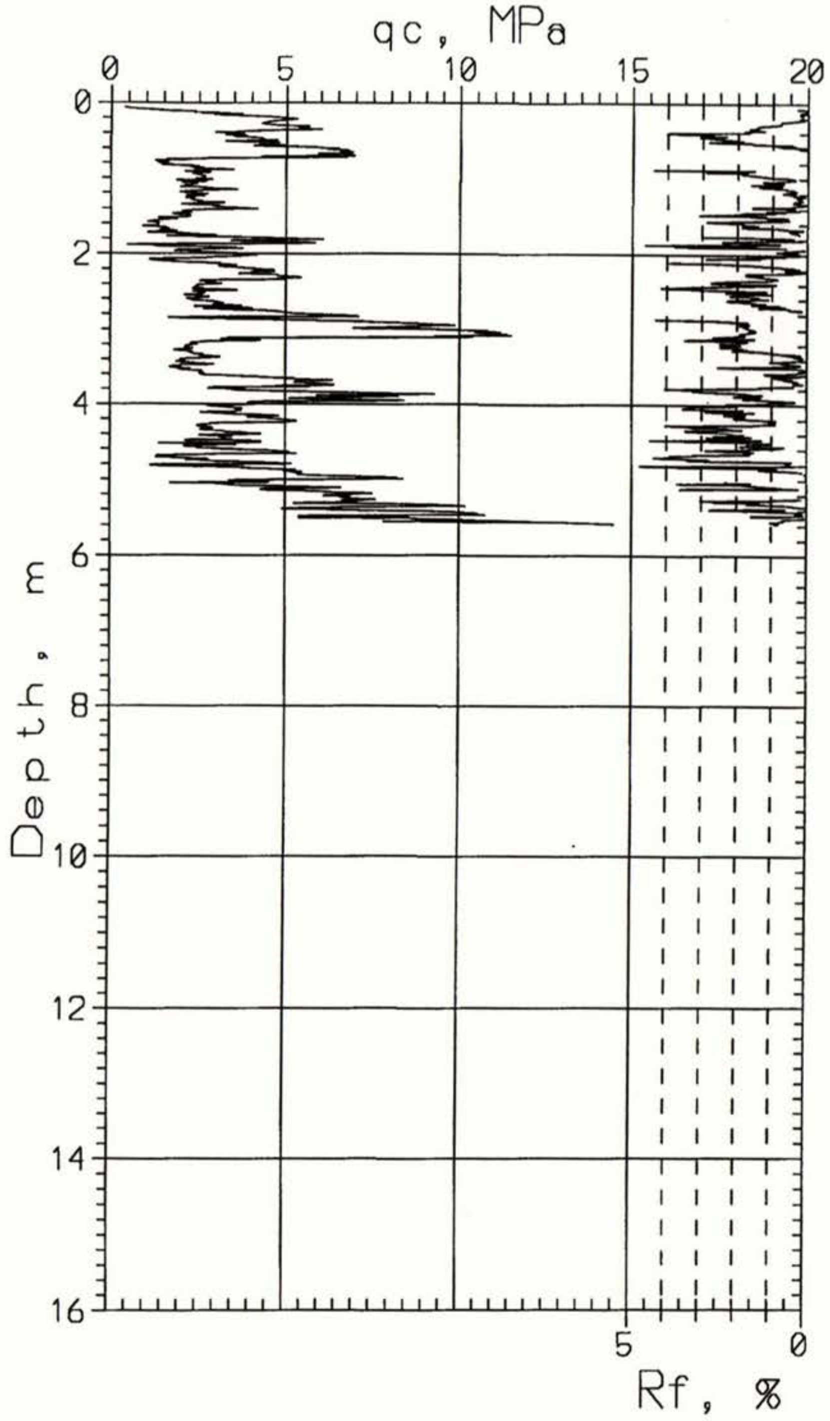

CPT test TEM005 28 May 1996

Appendix C: SPT test data.

CLIENT	Canterbury University	Ph: 3494-309 Canterbury Drilling Company
LOCATION	Jones Rd Gravel pit	
MACHINE	Williams	
TAKEN BY	DATE: 27/2/96	JOB FILE:	BORE LOG

Depth	Strata	Description of Soils	WL	SPT Blows / 75mm	Sampl
		BH1			
0–1m		Sandy Gravels		1/½/½/½/½/½	
1–2m		Sandy Gravels		1/½/½/½/1/½	
2–3m		Sandy Gravels		1/½/½/1/½/½	
3–4m		Sandy Gravels		2/2/1/1/1/2	
4–5m		Sandy Gravels		3/3/2/2/1/2	
		BH2			
0–1m		Sandy Gravels		½/½/½/½/½/½	
1–2m		Sandy Gravels		½/½/½/1/½/1	
2–3m		Sandy Gravels		1/1/1/½/½/1	
3–4m		Sandy Gravels		1/1/2/1/1/1	
4–5m		Sandy Gravels		1/2/2/1/1/2	